Chem Soc Rev

REVIEW ARTICLE

View Article Online
View Journal | View Issue

Cite this: *Chem. Soc. Rev.*, 2014, 43, 5896

Beyond post-synthesis modification: evolution of metal–organic frameworks *via* building block replacement

Pravas Deria,[a] Joseph E. Mondloch,[a] Olga Karagiaridi,[a] Wojciech Bury,*[ab] Joseph T. Hupp*[a] and Omar K. Farha*[ac]

Received 8th February 2014

DOI: 10.1039/c4cs00067f

www.rsc.org/csr

Metal–organic frameworks (MOFs) are hybrid porous materials with many potential applications, which intimately depend on the presence of chemical functionality either at the organic linkers and/or at the metal nodes. Functionality that cannot be introduced into MOFs directly *via de novo* syntheses can be accessed through post-synthesis modification (PSM) on the reactive moieties of the linkers and/or nodes without disrupting the metal–linker bonds. Even more intriguing methods that go beyond PSM are herein termed *building block replacement* (BBR) which encompasses (i) solvent-assisted linker exchange (SALE), (ii) non-bridging ligand replacement, and (iii) transmetalation. These one-step or tandem BBR processes involve exchanging key structural components of the MOF, which in turn should allow for the evolution of protoMOF structures (*i.e.*, the utilization of a parent MOF as a template) to design MOFs composed of completely new components, presumably *via* single crystal to single crystal transformations. The influence of building block replacement on the stability and properties of MOFs will be discussed, and some insights into their mechanistic aspects are provided. Future perspectives providing a glimpse into how these techniques can lead to various unexplored areas of MOF chemistry are also presented.

1. Introduction

Metal–organic frameworks (MOFs), also known as porous coordination polymers (PCPs), define a class of hybrid solids consisting of periodic coordination networks containing multitopic organic linkers and metal-ion-containing nodes or secondary building units (SBUs).[1–5] These crystalline, highly porous solids can possess ultra-high Brunauer–Emmett–Teller (BET) surface areas ($\sim$7000 m^2 g^{-1})[6–9] and thus have garnered much interest for gas capture, separation and storage.[10–17] However, the modular nature of the MOF structures, stemming from the tunability of the linker and metal SBUs, has also sparked interest in applications involving catalysis,[18–20] light harvesting,[21–25] sensing,[26] optical luminescence,[27,28] ionic conductivity,[29–32] and non-linear optical behavior.[33] Access to a wide range of potential applications is intimately tied to the ability to present a similarly wide range of chemical functionality within MOFs. Incorporation of functionality is straightforward if appropriately derivatized organic linkers can be synthesized and then directly employed in solvothermal materials syntheses. In some cases, however, challenges due to limited linker solubility, chemical stability, thermal stability, or functional group compatibility can preclude direct synthesis. Similarly, undesired reactions between linker functional groups and metal ions can lead to undesired products, to the exclusion of desired materials. Overly strong metal-ion–linker bonding can lead to formation of amorphous kinetic products to the exclusion of crystalline compounds.[34] Finally, undesired polymorphs of crystalline MOFs may be obtained to the exclusion of desired, and typically higher energy (*i.e.*, thermodynamically less stable), polymorphs.[35] These issues have been a limiting factor in MOF synthesis, which in turn has truncated the range of accessible chemical functionality that can be incorporated into MOFs.[36–38]

Post-synthesis modification (PSM), extensively reviewed by Cohen[38,39] and by Burrows,[40] effectively removes the potential for functional-group interference during MOF assembly. PSM involves heterogeneous chemical reactions to functionalize preassembled MOF structures[38,39] *via*:

(i) *modification of linkers* including (a) covalent modification (or elaboration), (b) deprotection of linker functionality (including demetalation),[38,39,41–44] and (c) electron addition (reduction) and concomitant incorporation of charge compensating ions.[45]

[a] *Department of Chemistry, Northwestern University, 2145 Sheridan Road, Evanston, Illinois 60208, USA. E-mail: j-hupp@northwestern.edu, o-farha@northwestern.edu*
[b] *Department of Chemistry, Warsaw University of Technology, Noakowskiego 3, 00-664 Warsaw, Poland. E-mail: wojbur@ch.pw.edu.pl*
[c] *Department of Chemistry, Faculty of Science, King Abdulaziz University, Jeddah, Saudi Arabia*

(ii) *modification of metal-containing nodes* including (a) incorporation of non-framework or pendant ligands *via* dative bonding to coordinatively unsaturated metal sites,[38,39,46–50] (b) alkyl or silyl grafting to oxygen atoms in metal-oxide nodes,[51,52] and (c) attachment of metal ions or complexes at node oxygen sites *via* atomic layer deposition (ALD)[53] or *via* reaction with organometallic species in dry solutions.[53,54]

Beyond these extensively studied PSM approaches, various conceptually different post-synthesis routes are now emerging. *Building block replacement* (BBR) involves replacement of key structural components of the MOF including (i) solvent-assisted linker exchange (SALE), (ii) non-bridging ligand replacement, and (iii) transmetalation at nodes or within linkers. (Fig. 1 shows some examples of MOFs used in the BBR processes discussed below.) BBR is intriguing given that it opens up a very broad strategy for the synthesis of isostructural MOFs that in turn should enable functional MOF chemistry. Both one-component and tandem building block replacement processes can provide access to otherwise unattainable MOF structures and functionality. They also may provide access to MOFs featuring gradient compositions and chemical properties.

Solvent-assisted linker exchange, (SALE),[55–57] often offers complete exchange of one organic linker for another possessing new functionality. Likewise, while transmetalation[58] provides a route to incorporate desired metal ions that are difficult to incorporate *via de novo* synthesis, replacement of non-bridging charge-balancing ligands represents an efficient way to engender new functional chemistry. In general, BBR reactions involve heterogeneous, linker, ligand, or metal-ion exchange, *via* breaking and remaking chemical bonds within the parent MOF.[55–59] Although it is difficult to be definitive, most examples of BBR to date appear to involve single crystal-to-single crystal transformations, rather than dissolution and recrystallization.

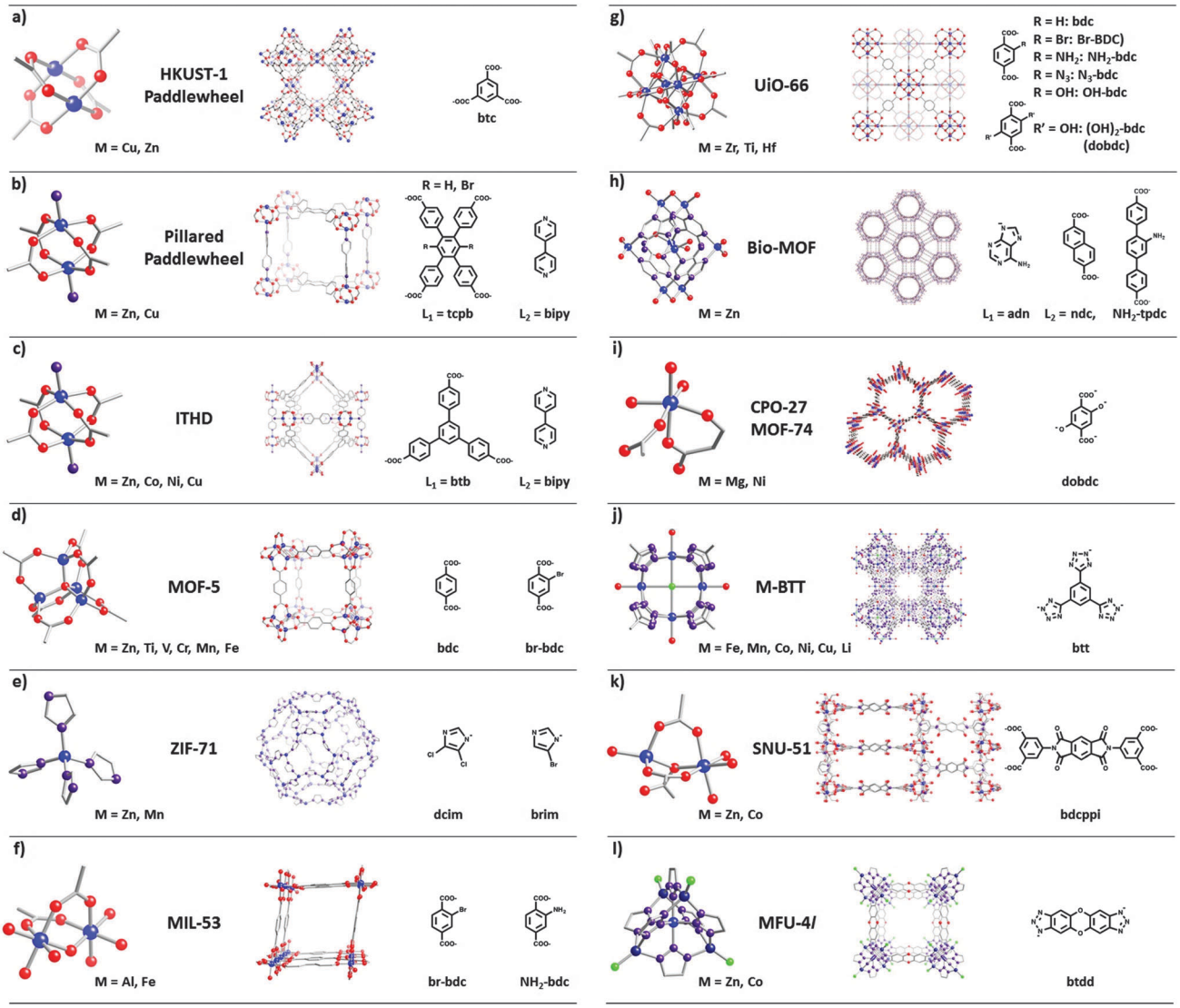

Fig. 1 Lattice structures (middle) and corresponding SBUs (metal nodes (left), and organic linkers (right)) of some of the MOFs discussed in this review. (Atom definition: blue – metal, red – oxygen, purple – nitrogen, grey – carbon, green – chlorine.)

Finally, in many cases it is relatively easy to find more mild conditions for BBR than the solvothermal conditions typically required for direct syntheses of MOFs. In our experience, BBR reactions also often work well with reactant concentrations that are too low for effective direct synthesis. Thus BBR can be especially useful when desired linkers or non-bridging ligands are expensive, delicate, or inherently incompatible with typical conditions for direct MOF synthesis.

BBR has been used to take on some recurring challenges in MOF synthesis, including: (i) preparing MOFs that appear to be inaccessible by direct methods; (ii) engineering the pores or nodes within MOFs (including controlling the pore volume, environment, aperture size, and chemical stability); and (iii) imparting or enhancing desired functional behaviour, including catalysis, selective gas sorption, ionic conductivity, redox conductivity, and mediating site-isolated chemistry. In addition, we discuss some of the key chemical factors controlling the extent, or even the feasibility, of BBR, both from the perspective of gaining a fundamental understanding and of discovering useful and transferable design or reaction rules. BBR reactions occurring only at or near the external surface of a MOF crystal[60–63] point to an intriguing further level of potential structural and functional complexity; however those studies are beyond the scope of the review. Finally, we briefly speculate on possible new ways in which BBR may prove synthetically or functionally useful.

2. Solvent-assisted linker exchange

While PSM is often effective for circumventing problems associated with direct MOF preparation (*vide supra*),[38,39] replacement of linkers is another viable strategy. It has variously been termed "stepwise synthesis",[64] "bridging linker replacement",[64] "post-synthetic exchange",[59] isomorphous ligand replacement,[65] and stepwise ligand exchange.[64] We prefer the term "SALE"[55–57,64–74] as it highlights the importance of the solvent during linker exchange. Conceptually SALE occurs at the solid–solution interface; a parent MOF is placed in a solution containing a second linker and a daughter MOF retaining the parent MOF topology is obtained. Similar linker exchange approaches have been utilized in metal diphosphonate-pillared zirconium phosphate,[75] cross-linked organophosphazene polymers,[76] and supramolecular coordination complexes, including metal–organic polyhedra,[77,78] but these are beyond the scope of this review.

2.1. Pore engineering

2.1.1. Controlling pore volume. Burnett *et al.* first demonstrated that SALE could be utilized to engineer the pore dimensions of a MOF.[64] Starting from 2-D (**PPF-18**) and 3-D (**PPF-20**) pillared-paddlewheel structures (consisting of Zn_2(**tcpp**) 2-D layers periodically linked with **dpni** pillars; see Fig. 1b for a related structure), Burnett *et al.* completely exchanged the 15.4 Å **dpni** pillars of **PPF-18** and **PPF-20** with 7.0 Å **bipy** pillars in a DEF–EtOH solution at 80 °C. The resultant frameworks, **PPF-27** and **PPF-4**, have significantly smaller pores when examined by single crystal X-ray diffraction (*e.g.*, c = 87.59 to 54.89 Å for **PPF-20** to **PPF-4**). A handful of additional papers utilizing MOFs of varying topologies (see Fig. 1 for example) have confirmed that SALE does in fact occur in the presence of linkers whose dimensions are smaller and/or of similar size to the linkers of the parent MOF.[55,59,74]

One might suspect smaller pore volumes to be readily obtainable *via* SALE—the diffusion of smaller linkers should be facile into pores of larger dimension (*vide infra*). In contrast, SALE of longer linkers might be significantly more difficult given presumably slower diffusion as well as the necessity for significant structural changes within the framework upon exchange. Recently however, Karagiaridi *et al.* demonstrated that linkers of increasing length could be introduced into the pillared-paddlewheel MOF, **SALEM-5** [Zn_2(**Br-tcpb**)(**dped**)], *via* SALE (Fig. 2).[56] **SALEM-5** contains layers of **Br-tcpb** linker and the 9 Å **dped** pillars which could be replaced by dipyridyl pillars of 11 Å **tmbbp** (**SALEM-6**), 14 Å **nbp** (**SALEM-7**) and 17 Å **tmbebp** (**SALEM-8**) (Fig. 2). In the most striking example (*i.e.*, **SALEM-5** with **dped** pillar to **SALEM-8** with **tmbebp** pillar), the c-axis of the resultant unit cell expands from 17.75 to 23.50 Å. Likewise, Rosi and co-workers demonstrated that SALE of longer linkers is possible in MOFs containing carboxylate linkers, specifically during the transformation of **Bio-MOF-101** (Fig. 1h), which consists of the zinc-adeninate clusters $(Zn_8(\mathbf{adn})_4O_2)^{8+}$ periodically linked with **ndc** linker), to **Bio-MOF-103** $(Zn_8(\mathbf{adn})_4O_2)^{8+}$ periodically linked with **NH_2-tpdc** linker).[79] In this series the unit cell was increased from 62.04 to 82.25 Å. Notably, most MOFs with increased pore volume could not be prepared *de novo*.

Framework catenation can also drastically change (diminish) MOF pore volumes. Bury *et al.* found that SALE could be used to access the non-catenated version of an otherwise catenated material. The SALE starting point was the non-catenated pillared-paddlewheel compound **DO-MOF** [Zn_2(**tcpb**)(**dped**); see Fig. 1b for a related structure].[67] **DO-MOF** contains 2-D sheets of the zinc-coordinated tetracarboxylate linker, **tcpb**, separated by the dipyridyl pillar, **dped**. In contrast, the **tcpb** linker with dipyridyl **bipy** and **abp** pillars yields two-fold catenated structures.

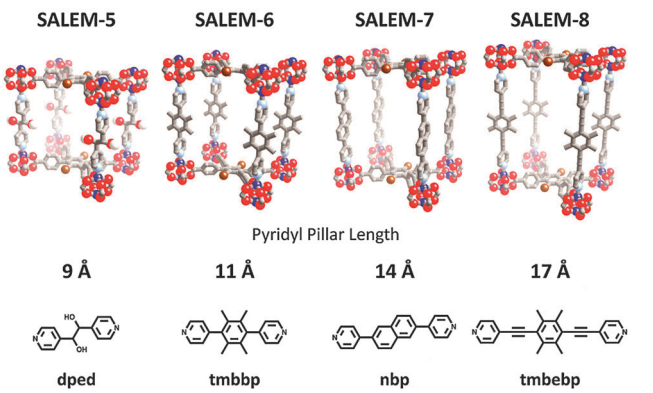

Fig. 2 Increasing pore sizes in an isoreticular series of pillared-paddlewheel MOFs synthesized *via* SALE. The value in Å represents the length of the dipyridyl linkers utilized for SALE on the parent MOF **SALEM-5**.

However, **DO-MOF**, under SALE conditions with **bipy** and **abp** replaces the **dped** pillars and yields the non-catenated MOFs containing **bipy** and **abp** ligands. Control over catenation was confirmed *via* thermogravimetric analysis as well as structural modelling *via* powder X-ray diffraction (PXRD). This study delineates an interesting alternative avenue to prepare non-catenated MOFs from those that exhibit catenation.

2.1.2. Controlling pore environment. The pore environment can also be readily controlled and modified *via* SALE. Kim *et al.* demonstrated that the **bdc** linker of **UiO-66** $[M_6O_4(OH)_4(\mathbf{bdc})_6]$ could be exchanged with **NH_2-bdc**, **Br-bdc**, **N_3-bdc**, **OH-bdc**, and **$(OH)_2$-bdc** (see Fig. 1g).[66] These exchanges could be observed both at the single particle level using aerosol time-of-flight mass spectrometry (ATOFMS) and on the bulk sample *via* ^{1}H NMR. ^{1}H NMR demonstrated that exchange ratios between 9 and 76% could be achieved depending on the solvent, temperature, and time of the reaction utilized. Interestingly, SALE can also occur between the preformed **NH_2-bdc** and **Br-bdc** MOF derivatives (*i.e.*, in a solid–solution–solid transformation).[59] These results suggest that one of the MOFs must dissolve to some extent for linker incorporation to occur.

Karagiaridi *et al.* also demonstrated that pore functionality could be readily controlled in another highly sought after class of MOFs, namely zeolitic imidazolate frameworks (ZIFs).[55] The **eim** linkers in $\{Cd(\mathbf{eim})_2\}$ (**CdIF-4**), a ZIF possessing RHO topology and Cd^{2+} nodes, could be exchanged for **nim** and **mim** linkers to form $\{Cd(\mathbf{nim})_2\}$ (**CdIF-9**), and $\{Cd(\mathbf{mim})_2\}$ (**SALEM-1**) respectively. The SALE reactions that occur between **CdIF-4**, **CdIF-9** and **SALEM-1** are summarized in Fig. 3. Importantly the studies from Kim *et al.*, as well as Karagiaridi *et al.*, demonstrate that some of the most robust MOF structures known are indeed amenable to SALE.

2.1.3. Controlling pore aperture dynamics through aperture modification. Controlling the pore aperture dynamics of MOFs is also achievable through SALE. By replacing the methyl group of the **mim** linker in **ZIF-8** $[Zn(\mathbf{mim})_2]$ for a hydrogen (**im** linker), Karagiaridi *et al.* demonstrated that an aperture along the *a*-axis in **SALEM-2** $[Zn(\mathbf{im})_2]$ is "opened up" (Fig. 4, from negligible to 2.9 Å).[57] It is important to note that the aperture of **ZIF-8** is dynamic[80] and it appears that these dynamics are more prevalent in **SALEM-2**. To probe the effect of this difference in pore aperture dynamics, **SALEM-2** and **ZIF-8** were exposed to solutions of *n*-hexane, cyclohexane, and toluene whose kinetic diameters are 4.3, 6.0, 6.1 Å respectively. As measured by TGA-MS, **SALEM-2** readily uptakes all three molecules while **ZIF-8** only displays uptake of *n*-hexane. The methyl group on the **mim** linker creates a steric hindrance of the 3.4 Å aperture (along the 111 axis) in **ZIF-8** which renders it less dynamic than that in **SALEM-2**.

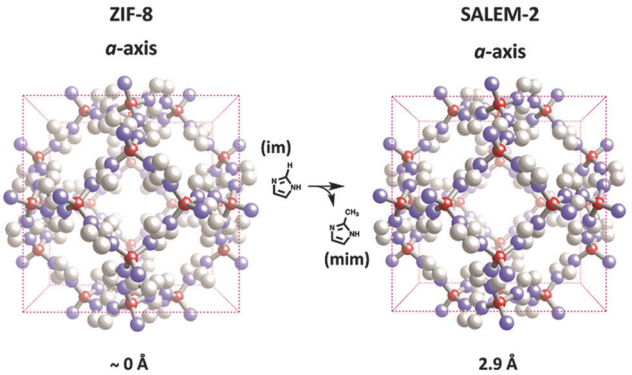

Fig. 4 Aperture modulation in **ZIF-8** through SALE.

2.2. Enabling functional MOF chemistry through SALE

2.2.1. Introduction of catalytically active sites. Porphyrin containing MOFs have been a highly sought after class of catalysts given their propensity to function as biomimetic analogues of metalloenzymes. Unfortunately in certain instances, designing MOFs with desired metalloporphyrins (*e.g.*, Co or Sn containing porphyrins[70]) can be extremely difficult under *de novo* synthetic conditions. Recently Takaishi *et al.* demonstrated that so-called robust porphyrinic MOFs (**M_1M_2-RPMs**), which contain 2-D sheets of tetracarboxylate metalloporphyrins (M_1) and porphyrin (free base or metalloporphyrin) containing dipyridyl pillars (M_2), could be subjected to SALE.[70] Starting from the **ZnZn-RPM** and utilizing a handful of dipyridyl containing linkers, Takaishi *et al.* successfully synthesized the following **M_1M_2-RPMs**: $Zn^{2+}2H^+$, $Zn^{2+}Sn^{4+}$, $Zn^{2+}Al^{3+}$, and $Zn^{2+}Co^{2+}$. Once in hand the Lewis acidic **ZnAl-RPM** was an active catalyst for the ring-opening of styrene epoxide with trimethylsilylazide (60% conversion). Notably the parent **ZnZn-RPM** only yielded 2% conversion under identical conditions.

Returning back to **UiO-66** (Fig. 1g), Pullen *et al.* utilized SALE to incorporate the linker FeFe(**dcbdt**)$(CO)_6$ into **UiO-66.**[73] The FeFe(**dcbdt**)$(CO)_6$ linker resembles the active site of known FeFe hydrogenase enzymes which are highly active H^+ reduction catalysts.[81,82] In combination with a photosensitizer ($[Ru(\mathbf{bpy})_3]^{2+}$) and a sacrificial electron donor (ascorbate) all under illumination, the FeFe(**dcbdt**)$(CO)_6$ containing **UiO-66** derivative is an active H_2 evolution catalyst (albeit largely at the surface of the MOF; Fig. 5). Pullen *et al.*'s results demonstrate the use of SALE to incorporate catalytically active moieties for the conversion of solar energy into useable chemical fuels within MOFs.

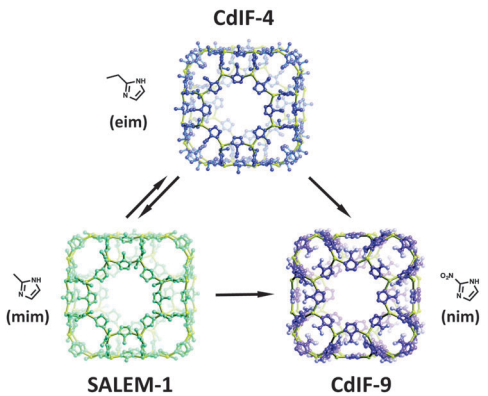

Fig. 3 Pore environment modification through SALE in ZIFs.

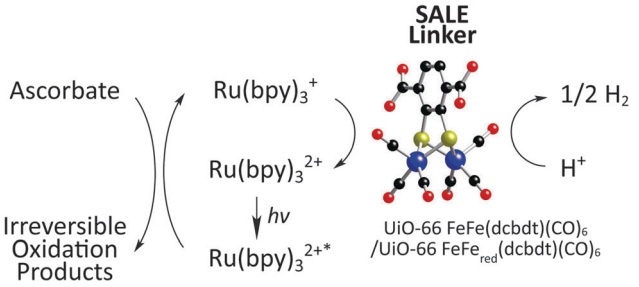

Fig. 5 Schematic representation of photocatalytic proton reduction process. The atoms in the linker utilized for SALE are defined as: red – oxygen, black – carbon, yellow – sulfur, and purple – Fe. Ru(**bpy**)$_3^{2+}$ and ascorbate were employed as photosensitizer and sacrificial electron donor, respectively.

2.2.2. Introduction of proton conducting sites. Kim *et al.* recently described the use of SALE to enhance proton conductivity within a MOF.[65] When **β-PCMOF2** [Na_3(**thbts**); Fig. 6], which has pores 5.6 Å in diameter and is lined with sulfonate oxygen atoms from a trianionic **thbts** linker, was exposed to the triprotic ligand H_3-**btp** a mixed ligand MOF, **β-PCMOF2½** [[Na_3(**thbts**)]$_{0.66}$[Na_3(H_3-**btp**)]$_{0.34}$(H_2O)$_{0.75}$] was obtained. **β-PCMOF2½** has pores partially lined with protonated hydrogen phosphonate groups (rather than the non-protonated sulfonate groups) that in turn facilitate the proton conductivity of **β-PCMOF2½**. A 1.5 orders of magnitude increase in conductivity relative to **β-PCMOF2** was observed. Furthermore, **β-PCMOF2½** is not accessible *de novo* and shows the highest equilibrated MOF proton conduction known to date.

2.2.3. Mediating chemical reactivity. Recently Vermeulen *et al.* described an elegant strategy for isolating ligands within MOFs and performing intramolecular olefin metathesis to create a molecule that otherwise could not be synthesized *via* metathesis.[72] Starting from a pillared-paddlewheel MOF {Zn_2(**Br-tcpb**)(**dpni**)} (**Br-YOMOF**), SALE was utilized to introduce a tetravinyldipyridyl pillar, resulting in **SALEM-14** (Fig. 7B). Subsequently, a first-generation Grubbs' catalyst was used to perform aromatic ring closing metathesis on the tetravinyl-pillar resulting in a new MOF, **PAH-MOF-1** (Fig. 7C). SALE proved to be necessary to avoid unproductive intermolecular chemistry and poisoning of the Ru-based catalyst by the Lewis basic pyridine. In short, the MOF was needed as a protecting reaction flask[83] to

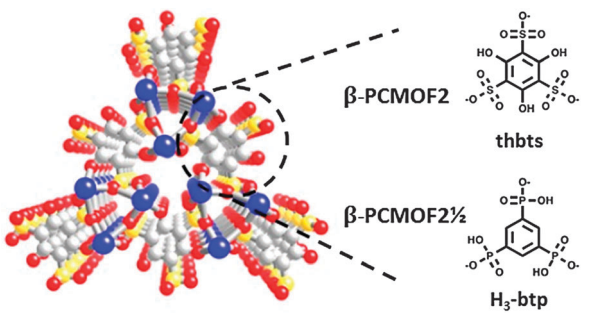

Fig. 6 Structure of **β-PCMOF2** and **β-PCMOF2½**. The atoms are defined as: blue – sodium, red – oxygen, grey – carbon, and yellow – sulphur/phosphorus.

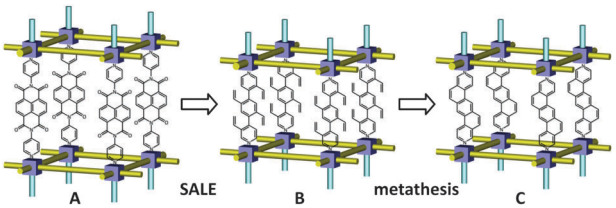

Fig. 7 Isolating reaction sites through SALE. SALE in **Br-YOMOF** (A) resulting in **SALEM-14** (B), where the isolated vinyl groups, followed by post-synthesis Grubbs catalysis reaction, provide **PAH-MOF-1** (C).

mediate the reaction, thus highlighting a potentially attractive avenue for MOF chemistry.

2.3. Feasibility of SALE: chemical principles

Recent experiments have given insight into some fundamental aspects of SALE. For most of the cases discussed above researchers have concluded that SALE is occurring in a single-crystal-to-single-crystal (rather than dissolution-reassembly) manner; however, more work is required to realize a complete mechanistic picture of SALE. As expected a fundamental understanding will take both thermodynamics (*e.g.*, pK_a of incoming linkers) and kinetics (*e.g.*, diffusion of linkers) into consideration and as expected the role of the solvent merits considerable attention.

2.3.1. Thermodynamic and kinetic aspects of linker exchange. The feasibility of linker exchange in MOFs should be carefully examined in light of its thermodynamics. In this regard, the reversibility of the exchange of **bdc** to **Br-bdc** linkers in the prototypical **MOF-5** [Zn_4O(**bdc**)$_3$, Fig. 1d], and its **Br-bdc** analogue has been studied recently by Gross *et al.*[69] Based on Gibbs free energy calculations for the **bdc**/**Br-bdc** ligand pair, the authors concluded that the ΔG associated with the linker exchange process in the **MOF-5** structure is approximately equal to zero, therefore the linker exchange can be regarded as an equilibrium between linkers in the solution and in the solid MOF crystals. In a one-step exchange process utilizing **MOF-5** with **Br-bdc** as an incoming linker at 85 °C they observed 15.2% (after 6 h) and 52.6% (after 24 h) incorporation of **Br-bdc**. However, when the exchange was performed on the **Br-bdc** analogue of **MOF-5** with **bdc** as an incoming linker, it was found that as much as 40.7% of the **Br-bdc** linker was replaced after 6 h. Moreover, it was also found that the linker exchange in **MOF-5** is reversible, as it was shown in a two-step process (exchange of **bdc** to **Br-bdc** and reverse). The significant difference in exchange ratios for **MOF-5** and its **Br-bdc** analogue was explained in terms of reaction kinetics; as the different sizes of the **bdc** and **Br-bdc** linkers affect the relative diffusion rates of incoming ligands during linker exchange (as **Br-bdc** substitutes into the **MOF-5** framework, the pore size is reduced due to the bulky **Br-bdc** molecules).

Another kinetic aspect that deserves evaluation is the role of crystallite size on the rate of SALE. In their work on RPM systems, Takaishi *et al.* experimented with varying the crystal size of the MOF by grinding and monitoring the rate of the reaction.[70] They discovered that the ground crystals reached

SALE equilibrium more rapidly than the larger crystals indicating the salient role of diffusion in the SALE process. This finding was further corroborated by scanning electron microscopy – energy dispersive X-ray spectroscopy (SEM-EDX), which established that the concentration of Sn (the metal present in the incoming metallo-porphyrin based dipyridyl pillars) was much higher around the crystal surface than in the crystal core.

2.3.2. pK_a correlations. In the course of SALE reactions the metal-parent linker bonds are broken and the metal–daughter linker bonds are formed. In the case of the nitrogen-based imidazolate and dipyridyl linkers, the pK_a of the conjugate acid (*i.e.*, the corresponding monoprotonated linkers) can be used as a measure for the strength of the coordination bond they would form with the metal; a higher pK_a results in more stable ligand–metal coordination. The sequential and reverse SALE studies performed on the previously described **CdIF-4** system (Fig. 3) glean some insight into this matter. It was observed that the single crystal-to-single crystal exchange of the **eim** and the **mim** linkers of **CdIF-4** and **SALEM-1** are possible. However, an attempt to perform SALE of **eim** or **mim** on {Cd(**nim**)$_2$} (**CdIF-9**) results in dissolution of the parent crystals rather than linker exchange (Fig. 3; note the reversibility of the SALE reactions).[55] This result was rationalized based on the relative Lewis basicity of the imidazolate derivatives in question. A lower basicity of the **nim** linker in comparison to **eim** and **mim** results in weaker Cd–N coordination bonds in **CdIF-9** than those present in the **CdIF-4** and **SALEM-1** compounds, respectively. Therefore, the crystals of **CdIF-9** most likely dissolve at a higher rate than the bonds between Cd and the incoming imidazolate are formed, resulting in framework dissolution. In a follow-up study, Karagiaridi *et al.* investigated the effect of the pK_a of the conjugate acids of monoprotonated dipyridyl pillars on the feasibility of a SALE reaction.[56] They exposed crystals of **SALEM-5** (Fig. 2) to a solution containing, in one case, equimolar amounts of **bipy** (pK_a = 4.44) and **tmbbp** (pK_a = 4.68), and in another case equimolar amounts of **bipy** and **abp** (pK_a = 3.62). In both cases, ^{1}H NMR spectra established selective SALE of the more basic linker. These studies also provide insight on the selection of both the parent MOF system and the incoming linker to be incorporated into it.

2.3.3. Solvent effects. SALE reactions requires solvent that enables linker dissolution and diffusion into the MOF interior. Though several SALE studies emphasize that the linker exchange is only feasible in one particular solvent (for example SALE of **im** into **ZIF-8** only takes place in *n*-BuOH),[57] the role of the solvent on SALE still remains unclear. One rigorous solvent study by Kim *et al.* reveals that the solvent polarity and coordinating ability play a key role during SALE of **bdc** derivatives within **UiO-66**.[59] The extent of SALE in various solvents increases in the order of chloroform < MeOH < DMF < water. This study also highlights the importance of careful solvent selection as it can have a profound effect on the solubility of the linkers that are being incorporated *via* SALE. For example, the solubility of **Br-bdc** in water is lower than that of **NH$_2$-bdc**, which translates into a lower extent of **Br-bdc** incorporation into **UiO-66** particles (48% *vs.* 67% with **NH$_2$-bdc**).

3. Non-bridging ligand replacement

While MOF nodes can be composed of single metal ions, they can also be comprised of discrete metal-containing clusters (see Fig. 1 for examples). These metal-cluster containing nodes offer an opportunity to introduce a battery of new functionality through the replacement of charge balancing non-bridging ligands. While typical metal node functionalization utilizes dative bonding to coordinatively unsaturated metal sites,[46–50] non-bridging ligand replacement relies on either acid–base or ligand exchange chemistry between the existing anionic ligand on the MOF node and the incoming anionic ligand. The result is the introduction of functional groups as charge compensating and strongly bound moieties to the MOF node *via* ionic bonding. Like SALE, non-bridging ligand replacement is expected to be governed by many of the factors that govern SALE including solvent selection, diffusion, and pK_a of the conjugate acids (*vide infra*).

This idea was recently realized when Deria *et al.* reported a new BBR technique called solvent-assisted ligand incorporation (SALI) for Zr-MOFs. The authors reported the efficient incorporation of carboxylate-based organic functional groups (CFGs) into the mesoporous MOF, **NU-1000** (Fig. 8a), consisting of $[Zr_6(\mu_3\text{-}OH)_8(\text{–}OH)_8]^{8+}$ nodes and **TBAPy** linkers.[84] The incorporation of new carboxylate based functionalities (CFGs) *via* SALI is encompassed by two boundary compositions of the Zr_6-node – $[Zr_6(OH)_{16}(RCOO)_8]$ – before functionalization, and $[Zr_6(O)_4(OH)_4(RCOO)_8(R'COO)_4]$ – after the SALI process, which is governed by an acid–base equilibrium between the carboxylic acid moiety of the incoming ligand (R′COOH) and a pair of hydroxyl ligands of the node (forming a water molecule as a by-product). Notably, carboxylates (R′COO$^-$) of weaker conjugate acids were found to be efficiently supplanted by those of stronger conjugate acids. Thus the distinctive feature of SALI, from a SALE reaction perspective, is that it does not involve replacement of a bridging linker, but instead a charge compensating and non-bridging ligand (*e.g.* hydroxide or a carboxylate ligand). The authors incorporated perfluoroalkane functionality

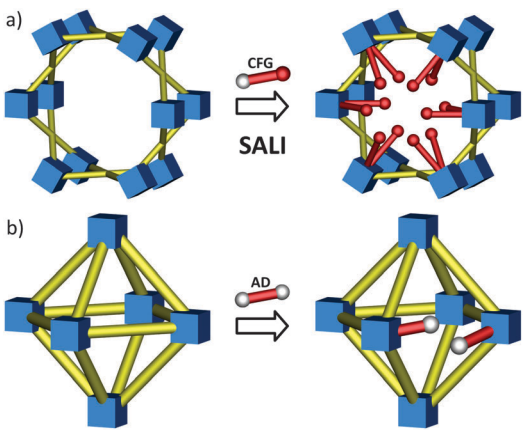

Fig. 8 Schematic representation of (a) solvent-assisted linker incorporation (SALI) with CFGs and (b) linker replacement with alkanedioic acids in various Zr-MOFs.

within the mesoporous channels of **NU-1000** by utilizing perfluoroalkyl carboxylic acids of varying chain length ($-CF_3$, $-C_3F_7$, $-C_7F_{15}$ and $-C_9F_{19}$). The resulting materials showed increased Q_{st} values for CO_2 and slightly less affinity for water vapor.[84] Notably, this technique not only proved to be versatile, tolerates many functionalities, but is also shown to yield new materials that are robust and effective for secondary functionalization at the SALI-incorporated moiety.[85]

In view of their high thermal, mechanical, and chemical stability,[86] **UiO-66**-type materials constitute a similarly intriguing class of MOFs compounds, considering a comprehensive picture regarding the stability and reactivity of this group of MOF materials. For instance, it was demonstrated by Wu *et al.*[87] and subsequently Katz *et al.*[88] that depending on the synthetic conditions the **UiO-66** framework (see Fig. 1g) may lack one or more structural elements[54] (*i.e.*, they may exhibit the missing linker phenomenon) without losing its integrity and topology; such systems can facilitate non-bridging ligand exchange. In a recent study, Suh and coworkers employed a slightly modified SALE approach to exchange the **bdc** linkers in **UiO-66** material for various flexible alkanedioic acids (AD).[89] As a result the authors obtained a series of modified **UiO-66-ADn** derivatives (Fig. 8b; **ADn** is defined as HOOC–$(CH_2)_n$–COOH, where n = 4, 6, 8, and 10). In contrast to a conventional SALE process, during the post-synthetic linker exchange, a single ditopic terephthalate linker (**bdc**) was replaced by two flexible ditopic alkanedioate ligands, leading to **UiO-66** derivatives functionalized with pendant carboxylic groups. Given that **UiO-66** materials can possess ''missing linker''-defects (for **UiO-66** consisting 12 linker nodes, a geometric surface area of 800 $m^2\ g^{-1}$ was estimated[88]), it is quite possible that a part of the AD-functionalization could proceed *via* a non-bridging hydroxyl ligand replacement (similar to that involved in SALI; *vide supra*) in addition to the **bdc** linker replacement process as described by the authors. Using ideal adsorption solution theory (IAST), they demonstrated that for landfill gas separation (a 50 : 50 mixture of CO_2 and CH_4), all of the **UiO-66-ADns** showed higher selectivity for CO_2 over CH_4 relative to **UiO-66**.

4. Transmetalation

In this section we will discuss reactions that involve post-synthesis replacement of MOF building blocks *via* transmetalation.[58] Also known as ''metal metathesis''[90] or ''metal-ion exchange'',[91] transmetalation entails partial or complete replacement of the metal nodes (or sometimes extra-framework metal moieties) of a MOF by a reaction with a metal precursor (in most cases a solution of a metal salt) in a single crystal-to-single crystal fashion. The emergence of this synthetic pathway in MOFs has been relatively recent, with around thirty reports of successful cases;[41,62,63,66,68,90–112] (including a few examples of complete replacement). Besides discussing how transmetalation engenders new MOF evolution and enables new functional chemistry, we analyze the current literature in order to provide a set of fundamental principles that govern successful metal replacement reactions. These principles appear to offer insight into why only a handful of transmetalation experiments lead to full metal exchange, whereas partial transmetalation is more common.

4.1. Metal node engineering

4.1.1. Obtaining compounds that are unattainable *de novo*. Perhaps the most straightforward and obvious aspect of transmetalation is its ability to generate MOFs featuring metals that are challenging to obtain for specific compounds through conventional syntheses. This is especially relevant in the case when a new structurally or functionally interesting MOF topology is synthesized with a given metal node. Attempts to diversify a specific MOF by adapting an established synthetic pathway to other metal ions are not always successful, since the variation in size, geometric restriction on the preferred coordination sphere and electronic properties of the different metal ions may interfere with the MOF structure assembly. For instance, Prasad *et al.* prepared {[Zn_2(**bdcppi**)$(DMF)_3$] × 6 DMF × $4H_2O$} (**SNU-51**), a Zn^{2+}-based MOF of PtS topology (Fig. 1k); however, when they employed Cu^{2+}, under similar synthetic conditions the resulting product crystallized in the NbO topology {[Cu_2(**bdcppi**)$(DMF)_2$] × 10DMF × $2H_2O$}.[91] In an attempt to prepare **Cu-SNU-51**, the authors employed transmetalation by soaking **Zn-SNU-51** in a methanolic $Cu(NO_3)_2$ solution. While powder X-ray diffraction (PXRD) established that the parent and daughter materials are structurally similar and no new phase was formed, the authors ruled out the recrystallization following a dissolution process based on the fact that the transmetalation rate was fast (27%, 44% and 75% conversion in 10, 30 and 120 minutes respectively) as followed *via* ICP analysis. It is important to note that more information regarding the rates of single crystal-to-single crystal transmetalation as well as dissolution followed by recrystallization are needed to establish the true nature of these processes. The authors also found that no transmetalation occurred when they attempted transmetalation of Cu^{2+} with Zn^{2+} on the Cu^{2+}-exchanged **Cu-SNU-51**. Likewise, in the presence of various other transition metal ions, such as Co^{2+}, Ni^{2+}, and Cd^{2+}, the Zn^{2+}-based **SNU-51** only transmetalated with Cu^{2+} in a solvent-dependent manner indicating that *thermodynamic stability of the daughter framework is a key driver for transmetalation*, *where solvent governs other crucial aspects including solubility, coordinating ability and the effective solvation shell of a metal ion*.

Similarly, attempts *via* conventional solvothermal syntheses to create Cu^{2+}, Co^{2+} and Ni^{2+} analogues of {[Zn_7(**btt**)$_3(H_2O)_7]_n$–[Zn_5(**ppbotctc**)$_3(H_2O)_5]_n$}, a unique interpenetrated cationic/anionic polyhedron-based double framework with square pyramidal, triangular-pyramidal, octahedral and triangular-paddlewheel Zn^{2+} nodes were unsuccessful;[105] so were the efforts of Denysenko *et al.* to synthesize a Co^{2+}-based **MOF-5**-like structure {Zn_5Cl_4(**btdd**)$_3$} (**MFU-4*l***; Fig. 1l) with large **btdd** linkers that they had obtained for Zn^{2+}.[94] To avoid tedious optimization, all the above research teams utilized transmetalation to successfully achieve their goals.

Certain metal ions are particularly challenging to incorporate into MOFs under standard solvothermal synthesis conditions. One set of examples consists of various elements in low-oxidation states – for example, Ti^{3+}, V^{2+} and Cr^{2+}. Standard solvothermal synthesis conditions (at elevated temperatures in the presence of air) often induce their oxidation.[93] Small metal cations such as Ti^{4+} pose difficulties when it comes to incorporating them into structures that demand high coordination numbers, such as the $\{M_6O_4(OH)_4(CO_2)_{12}\}$ cluster of **UiO-66** (see Fig. 1g).[66] Conversely, it is not trivial to introduce metals that favor unusually high coordination numbers, *e.g.*, lanthanides, into the low-density sodalite topology of $\{M_3[(M_4X)_3L_8]\}$ (where metals are found in an octahedrally coordinated geometry; see Fig. 1j, and X = Cl or O and L = **btt** or **hett**).[90] As discussed in more detail below, transmetalation has in several instances proven to be an effective way to meet these challenges and has helped expand the synthetic possibilities in MOF chemistry.

4.1.2. Transmetalation to Ni^{2+} for increasing stability and improving accessible porosity. Accessing the porosity of many low-density MOFs towards gas molecules has been a significant challenge. Interestingly, even when the evacuation of solvent molecules from the framework does not eliminate MOF crystallinity, loss of porosity may still be observed. Possible reasons for the loss of porosity include channel collapse during solvent removal, pore blockage due to residual solvent,[113,114] and/or degradation of crystal surfaces as the exposed terminal linkers bound to metal ions can sometimes be lost (*i.e.*, replaced by solvent);[97] MOFs possessing metal ions (*e.g.*, Mg^{2+}, Zn^{2+} *etc.*) with weaker metal–linker bonds (*vide infra*) can be vulnerable to degradation. Though exchanging to a low boiling solvent followed by its removal under mild conditions[36] or employing supercritical CO_2 activation[115] often provide access to high surface area MOFs, transmetalation of MOFs with metal ions that form stronger metal–linker bonds can also provide access to high surface areas and permanent porosity. In octahedral environments, Ni^{2+} typically forms stronger bonds to anionic oxygen species (*e.g.*, from carboxylate) than does Mg^{2+} and often displays a thermodynamic preference for octahedral coordination (*vide infra*); therefore, transmetalating MOFs with octahedrally coordinated metal nodes to Ni^{2+} ions can result in improved stability, engendering accessibility to higher porosity. Kahr *et al.* subjected **Mg-MOF-74**, with the general formula $\{M_2(\mathbf{dobdc})\}$ (Fig. 1i), to varying degrees of transmetalation of Ni^{2+} (in the range of 10–70%).[97] Unlike the parent MOF, which required prolonged solvent exchange to achieve a N_2 uptake of 18 mmol g^{-1}, these Ni^{2+} exchanged, mixed-metal (Mg–Ni) materials adsorbed up to 13 mmol g^{-1} N_2 after conventional thermal activation (note that the parent **Mg-MOF-74** and **Ni-MOF-74** showed respective N_2 uptake of 0.5 mmol g^{-1} and 12.5 mmol g^{-1} upon similar thermal activation process[116]). Song *et al.* observed similar results with their **ITHD** MOF system with the general formula of $\{M_6(\mathbf{btb})_4(bipy)_3\}$ (Fig. 1c).[63] Whereas the Co^{2+} and Zn^{2+} analogues required activation *via* supercritical CO_2 drying to access their porosity, the Ni^{2+}-exchanged product demonstrated a BET surface area of 5590 m^2 g^{-1} just by conventional vacuum drying activation – one of the highest BET surface areas reported without activation *via* supercritical CO_2 drying (by comparison, the Zn^{2+} analogue was nonporous and the Co^{2+} analogue only showed a BET surface area of 480 m^2 g^{-1}, upon similar vacuum activation). Therefore, transmetalation to Ni^{2+} can be used to stabilize an attractive MOF structure towards gas sorption.

4.2. Introducing new chemical functionality in MOFs *via* transmetalation

4.2.1. Synthesis of redox-active MOFs and catalysis. MOFs endowed with redox-active properties could prove valuable for both chemical and electrochemical catalysis. However, decorating MOFs with redox-active metals is not an easy task due to the vulnerability of cations in lower oxidation states towards oxidation (*vide supra*) during *de novo* synthesis. Sub-stoichiometric transmetalation allowed Brozek *et al.* to produce seven **MOF-5** (Fig. 1d) analogues featuring Ti^{3+}, V^{2+}, V^{3+}, Cr^{2+}, Cr^{3+}, Mn^{2+} and Fe^{2+} ions (Fig. 9).[93] Using $NOBF_4$, the authors successfully oxidized Cr^{2+} to Cr^{3+} in **Cr-MOF-5.** An inner-sphere oxidation of Fe^{2+} to Fe^{3+} in **Fe-MOF-5** by coordinated NO was demonstrated to highlight the redox activity of the transmetalated products. Likewise, the partially Co^{2+}-exchanged MOF **MFU-4*l*** (Fig. 1l) described earlier also exhibits redox activity, as it undergoes reversible oxidation by oxygen and catalyzes gas-phase oxidation of CO to CO_2.[94]

Transmetalation offers an attractive strategy for the incorporation of catalytically active metal centers in MOF linkers. The synthesis of catalytic MOFs featuring salen-[41] or porphyrin-based[104] linkers has particularly benefitted from this approach. Shultz *et al.* were able to expand a family of M-salen-containing pillared-paddlewheel **MSO-MOF** materials $[Zn_2(\mathbf{tcpb})(\mathbf{salen})]$ by a stepwise replacement of Mn^{3+} in the salen linker with Co^{2+}, Zn^{2+}, Cr^{2+}, Cu^{2+}, Ni^{2+} or Mn^{2+} (Fig. 10b) resulting in a series of potential catalysts.[41] Similarly, Zhang *et al.* applied transmetalation to their "ship-in-a-bottle" material **porph@MOM-10**, a [*meso*-tetra(*N*-methyl-4-pyridyl)porphine tetratosylate] encapsulated in the $\{Cd_6(\mathbf{bpt})_4Cl_4(H_2O)_4\}$ framework, which contains catalytically inactive Cd^{2+} ions both in its nodes and in the porphyrin moiety.[104] Replacement of Cd^{2+} throughout the material with Mn^{2+} afforded a product (Fig. 10a) that could catalyze the epoxidation of *trans*-stilbene with 75% conversion (compared to only 7% conversion provided by the original Cd^{2+} containing **porph@MOM-10**). Notably, the Mn^{2+} analogue proved inaccessible *de novo*.

4.2.2. Effects of transmetalation on gas sorption. The earliest report on MOF transmetalation appears to be that of Dincă *et al.* who experimented with replacing the Mn^{2+} centers

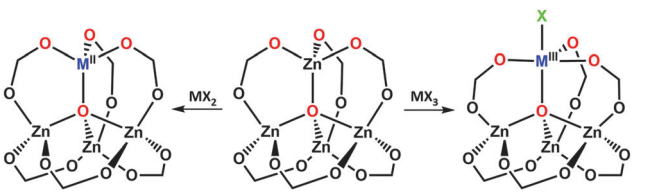

Fig. 9 Partial transmetalation in Zn_4O node within **MOF-5**.

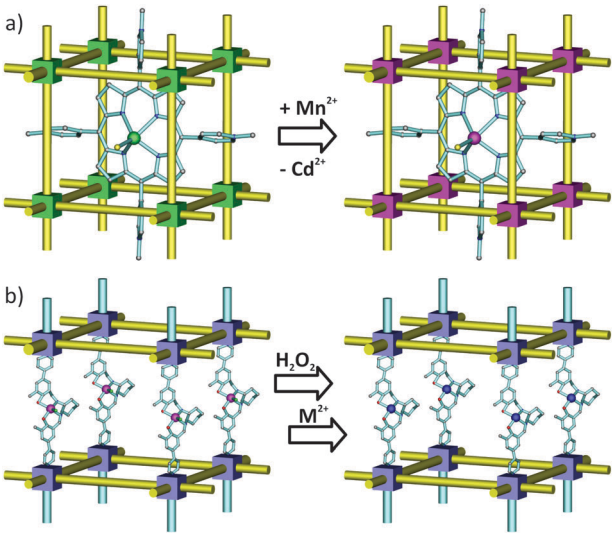

Fig. 10 Transmetalation in (a) **porph@MOM-10**, and (b) **MSO-MOF**. Note that for the panel (b), the metalation was carried out after the demetalation of the parent MOF in a sequential manner.

in $\{Mn_3[(Mn_4Cl)_3(\mathbf{btt})_8(CH_3OH)_{10}]_2\}$ (**M-btt**; Fig. 1j) with Li^+, Cu^+, Fe^{2+}, Co^{2+}, Ni^{2+}, Cu^{2+} and Zn^{2+}. Their aim was to elucidate the role of coordinatively unsaturated metal centers in enhancing hydrogen uptake and altering Q_{st}.[95] In most cases the displaced ions were the extra-framework Mn^{2+} ions; for example, Fe^{2+} and Co^{2+} each replaced 100% of the extra-framework Mn^{2+} species (including incorporation of an additional equivalent of Fe^{2+} or Co^{2+} as a charge-balancing extra-framework ion). Ni^{2+} could replace ~90% of Mn^{2+}, and the incorporation of Li^+ and Cu^+ was minimal. Notably, in the case of Cu^{2+} and Zn^{2+}, partial replacement of intra-framework metal nodes was also observed. These studies revealed several interesting trends. The authors observed an increase in Q_{st} for H_2 sorption in these transmetalated MOFs going from Mn^{2+} to Fe^{2+} to Co^{2+}, which they attributed not only to a decrease in the ionic radius of the incorporated metal ions, but also to the presence of an increasing amount of additional extra-framework cations. Furthermore, they obtained relatively low Q_{st} values for the monovalent Li^+ and Cu^+ species; nevertheless, the Cu^+ analog exhibited a surprisingly high Q_{st} despite minimal Cu^+ incorporation: for the Li^+ analogue, a Q_{st} value of 8.9 kJ mol^{-1} was measured with a Li/Mn ratio of 0.017 : 1.000, whereas for the Cu^+ analogue, a higher Q_{st} value of 9.9 kJ mol^{-1} was measured even with an extremely low Cu/Mn ratio of 0.028 : 1.000 (note that for the parent material with Mn^{2+}, a Q_{st} of 10.1 kJ mol^{-1} was measured). This transmetalation study enabled the authors to measure, for the first time, the Q_{st} values associated with hydrogen binding to Fe^{2+} and Ni^{2+} ions. The work of Dincă *et al.* demonstrates the wealth of information that can be obtained from studying isostructural MOFs functionalized by different metal ions – a goal that can be readily achieved by transmetalation, given its single crystal-to-single crystal nature.

Transmetalation has also been implemented for the improvement of CO_2 sorption properties. It has been recently shown that the Zr^{4+} nodes of the highly robust **UiO-66** (Fig. 1g) can be partially transmetalated with the significantly smaller cation Ti^{4+}.[66] Lau *et al.* demonstrated that modification of the **UiO-66** framework leads to pore constriction that promotes better accommodation of CO_2 molecules, and which is ultimately manifested in an enhancement of the CO_2 uptake.[96] In fact, replacing only 56% of the heavy Zr^{4+} nodes with Ti^{4+} led to an 80% improvement of the framework's ability to take up CO_2 (from 2.3 mmol g^{-1} to 4 mmol g^{-1} at 120 kPa). Notably, this enhancement of the gravimetric CO_2 uptake is much higher than that expected from reduction of the molecular weight of the MOF (calculated to be 19% for a model of a 100% Ti^{4+}-exchanged **UiO-66**). Botas *et al.* also observed a similar improvement in CO_2 uptake – in partially Co^{2+}-doped **MOF-5**.[112] They attributed this effect to an increase in charge–quadrupole interactions between the doped framework and CO_2.

4.2.3. Sensing. When MOF transmetalation occurs in a specific and easily detectable fashion, it can be exploited for sensing metal cations. This idea was used in the case of the fluorescent **Al-MIL-53** MOF with the general formula of {M(OH)(**bdc**)} (Fig. 1f). The MOF's fluorescence has been attributed to photo-emission from a ligand-to-metal charge transfer (LMCT) transition.[117] However, given the extraordinary energetic difficulty of accomplishing one electron reduction of Al(III), the attribution seems unlikely. Presumably emission is instead occurring from a linker-localized excited state. After Kim *et al.* demonstrated the feasibility of transmetalation in **Al-MIL-53** to Fe^{3+},[66] Yang *et al.* examined the application of this phenomenon to the detection of Fe^{3+} ions in solution.[117] It was found that the incorporation of Fe^{3+} quenches the emission. The resulting quenching of the fluorescence enables the detection of Fe^{3+} ions in the 3–200 μm concentration range.[118] The transmetalation happens exclusively between Al^{3+} and Fe^{3+}, possibly due to the similarity in their crystal radii (67.5 pm for Al^{3+} and 69.0 pm for low spin Fe^{3+} in a 6-coordinate environment),[119] with no interference stemming from the presence of cations such as Cu^{2+}, Na^+, K^+, Ni^{2+}, Ca^{2+}, Pb^{2+}, Mn^{2+}, Co^{2+}, Cr^{3+}, Hg^{2+}, Cd^{2+}, Zn^{2+}, Mg^{2+}, Fe^{2+}.

4.3. Feasibility of transmetalation: fundamental principles

Numerous examples of transmetalation in MOFs allow us to analyze its scope and feasibility to draw a more detailed picture regarding the fundamental processes involved. Below we provide an analysis of the most important factors that determine the success of transmetalation.

The first aspect to consider is the thermodynamic stability of the daughter MOF relative to the parent framework. To probe the stability of MOF nodes, we can resort to a criterion developed for transition metal complexes – the Irving–Williams series. The Irving–Williams series predicts increasingly stronger metal–ligand interactions in high-spin octahedral complexes of 3d M^{2+} species. The stability of the respective complex peaks for Cu^{2+}, then drops for Zn^{2+} since its fully occupied d orbitals do not experience additional crystal field stabilization. The Irving–Williams series nicely correlates with the stability of MOFs featuring octahedral metal centers (*e.g.*, MOFs with paddlewheel-based

structural building units). Many transmetalation studies report the feasibility of performing a transmetalation to Cu^{2+}. For example, Prasad *et al.* successfully replaced the Zn^{2+} centers in the previously described material **SNU-51** with Cu^{2+}.[91] Similarly, Zhang *et al.* inserted Cu^{2+} into the 2D material $\{Na_{0.25}[(CH_3)_2NH_2]_{1.75}[Cd(\mathbf{hmcem})_2]\}$ *via* replacement of the Cd^{2+} nodes.[102] Interestingly, Cu^{2+} tends to be the only ion capable of replacing the otherwise difficult intra-framework metal nodes in the case of the aforementioned $\{Mn_3[(Mn_4Cl)_3(\mathbf{btt})_8(CH_3OH)_{10}]_2\}$ and **MSO-MOF** systems.[41,95]

The applicability of the Irving–Williams series to assess MOF stability is especially evident in studies that focus on comparing the feasibility of transmetalation by different metal species. Zhang *et al.* observed that their attempts to replace zinc ions in the double polyhedron $[Zn_7(\mathbf{btt})_3(H_2O)_7]_n$–$[Zn_5(\mathbf{ppbotctc})_3(H_2O)_5]_n$ with Cu^{2+}, Co^{2+} or Ni^{2+} were only successful for Cu^{2+}.[105] Mukherjee *et al.* synthesized a 2D network $[\{[Zn(\mathbf{btin})_2(H_2O)_2]\cdot 2PF_6\ \text{pyrene}\cdot 2(H_2O)\}_n]$ of Kagomé dual topology with octahedral Zn^{2+} centers and performed an extended transmetalation study on it: the results of the study indicated that the compound could be rapidly transmetalated with Cu^{2+} or Cd^{2+}, with the Cd^{2+} nodes subsequently able to be transmetalated to Cu^{2+}; transmetalation of Cu^{2+} to Cd^{2+}, on the other hand, proceeded very slowly, whereas the transmetalation of Cu^{2+} to Zn^{2+} proved not feasible.[99] Reverse and serial transmetalation experiments conducted independently by Yao *et al.* and Song *et al.* on the paddlewheel-based MOFs **SUMOF-1** with the general formula of $\{M_6(\mathbf{btb})_4(\mathbf{bipy})_3\}$ (where $M = Zn^{2+}$) and the **ITHD** series (Fig. 1c), respectively, establish the thermodynamic stability trend in MOF metal nodes to be in the order $Cu^{2+} \gg Ni^{2+} > Co^{2+} \approx Zn^{2+}$, which is in good agreement with the Irving–Williams series (Fig. 11).[63,101] These results, along with the recorded data indicating strong Ni–O bonds and large formation constants for Ni–ammine complexes,[120] can explain the choice of Ni^{2+} in transmetalation experiments geared to enhance the framework stability (*vide supra*).

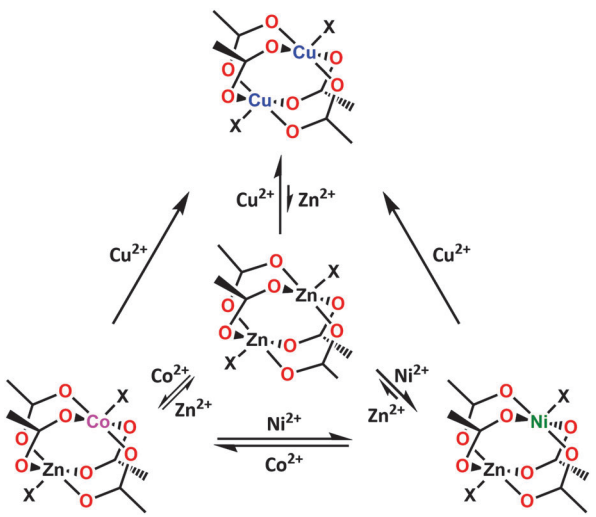

Fig. 11 Feasibility of partial *vs.* complete transmetalation for the first row transition metal ions, M^{2+}, in paddlewheel nodes showing a trend parallel to the stability of Irving–Williams series.

Another aspect governing transmetalation is the preferable coordination state that a given metal assumes. For example, it is well known that Ni^{2+} favors octahedral coordination, unless it is coerced into a tetrahedral geometry by sterically demanding linkers. Consistent with these ideas, incorporation of Ni^{2+} into the Zn_4O cluster of **MOF-5** (which requires tetrahedral coordination of metal centers) has proven challenging. Brozek *et al.* observed that even after prolonged soaking of **MOF-5** in a Ni^{2+} solution, the extent of transmetalation was no more than 25%, meaning that, on average, only one Zn^{2+} per cluster was replaced uniformly by Ni^{2+} (Fig. 9).[92] Furthermore, inside the **MOF-5** cluster the Ni^{2+} ion assumes an octahedral geometry by coordinating to two DMF molecules, as evidenced by UV-Vis spectroscopy – becoming four-coordinated only following heating. Similar results were earlier reported for Co^{2+} doped **MOF-5**, again with only one Zn^{2+} ion per node being substituted by Co^{2+}.[112] Partial metal exchange has also been observed for **MFU-4*l***, a material topologically related to **MOF-5**.[94] The pentanuclear node of **MFU-4*l*** consists of two types of Zn^{2+} metal centers, four outer tetrahedral metals and one inner octahedral metal. Although outer zinc ions can be replaced, even under forcing conditions Co^{2+} does not supplant the central, six-coordinated zinc ion, which results in the Co : Zn molar ratio of 4 : 1 in the exchanged material.

Finally, the success of transmetalation depends on the ability of the metal ion to access the framework interior. There is good evidence that rates of transmetalation can be limited by diffusion. For example, in some cases of partial transmetalation higher degrees of transmetalation have been measured at and near the MOF crystal exterior surface than in the interior.[62] Thus, a MOF must possess channels that enable diffusion of the incoming metal species to the crystal core. **MFU-4** $[Zn_5Cl_4(\mathbf{bbta})_3]$, which possesses very narrow (2.5 Å) pores was found to be impermeable to Co^{2+}, unlike its larger counterpart, **MFU-4*l*** [*i.e.*, $Zn_5Cl_4(\mathbf{btdd})_3$], which features 9.2 Å pores and successfully undergoes transmetalation as discussed above.[94] Additionally, pore flexibility may also facilitate the entry of metal ions. When transmetalation experiments with Cu^{2+} were performed on **Zn-HKUST-1** (Fig. 1a), a paddlewheel-based MOF with relatively small and rigid **btc** linkers, replacement was only 56% complete even after 3 months. In contrast, **Zn-PMOF-2** $[Zn_4(\mathbf{tdpeb})_8(H_2O)_{12}]$, another paddlewheel-based framework possessing more flexible **tdpeb** linkers, underwent complete transmetalation in three days.[62]

5. Outlook and future directions

In previous sections we discussed numerous examples of BBR, where only one structural element, namely the metal ions, charge-balancing ligands in the node or the organic linkers had been replaced. These examples nicely demonstrate that MOF structures are highly modular and can be altered *via* BBR. Recently presented strategies for tuning the physical and chemical properties of porous crystalline materials emphasize a deliberate introduction of framework heterogeneity by

increasing the number of constituents. Introducing a variety of building units into a single crystalline solid containing gradients of functionality may open up new opportunities for application-based MOF chemistry. This goal can be achieved, to some extent, by using *de novo* approaches – for example, incorporating multiple linkers into the same crystal containing different functional groups.[37,121]

Importantly, some recent examples demonstrate a high potential for the construction of multiple building block (nodes and the organic linkers) MOFs by utilizing the BBR strategy. An important exploration of BBR reactions towards multiple building block MOF structures is a stepwise replacement of linkers and metal ions in nodes within the parent framework. Cohen and co-workers selected two ZIF materials, zinc 4,5-dichloro-imidazolate {**Zn(dcim)$_2$**} (**ZIF-71**) with RHO topology (Fig. 1e) and zinc 2-methylimidazolate {**Zn(mim)$_2$**} (**ZIF-8**) with SOD topology (Fig. 4) for tandem building block replacement experiments (Fig. 12).[68] The exchange process for **ZIF-71** was conducted in two ways; in the first, the compound was exposed to a solution of 4-bromoimidazole (**brim**) for linker exchange, and then the metal cation was exchanged by soaking the brominated ZIF in a methanolic solution of Mn(acac)$_2$. For the reverse process, the exchange of a metal ion (Zn^{2+} to Mn^{2+}) was followed by the linker exchange (**dcim** to **brim**). After 3 days of incubation of **ZIF-71** in a methanolic solution of **brim**, ~35% of the **brim** had been incorporated into **ZIF-71**. Consecutive treatment of the obtained **ZIF-71(dcim/brim)** powder with Mn(acac)$_2$ in MeOH, resulted in bimetallic and multifunctional **ZIF-71(dcim/brim)-(Zn/Mn)**, where ~12% Mn^{2+} could be observed as a result of the metal exchange. The uniform distribution of linkers and metal centers in **ZIF-71(dcim/brim)-(Zn/Mn)** was further confirmed by SEM-EDX mapping. Additionally, ATOFMS indicated that the microcrystalline particles of the resulting material indeed contain the multiple building block **ZIF-71(dcim/brim)-(Zn/Mn)**. The tandem BBR experiment performed in the reverse order gave a nearly identical result, yielding the analogous **ZIF-71(Zn/Mn)-(dcim/brim)**, which contained ~12% Mn^{2+} and 30% **brim**. These results nicely demonstrate that tandem building block replacement is capable of incorporating a variety of building blocks into a single protoMOF.

While sequential transmetalation[63,101] and SALE[56,79] are known separately, Cohen's work provides the first example of sequential metal and linker replacement in the same system, which nicely illustrates the synthetic potential of BBR for the introduction of functional variety into MOF scaffolds. Looking forward, another interesting possibility for BBR would be the complete conversion of a protoMOF structure into a new material with new nodes and linkers by tandem building block replacement.

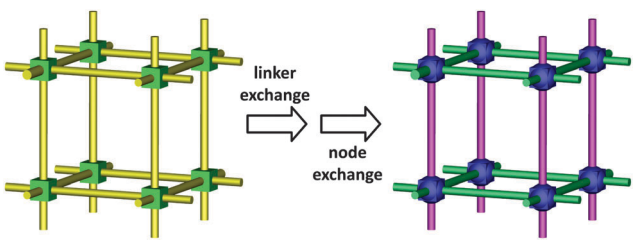

Fig. 12 Accessing multiple building block MOF *via* sequential building block replacements.

Like selective transmetalation, facilitated by the difference in metal–linker interactions, selective replacement of specific linkers *via* SALE in MOFs with multiple but similar linkers (*e.g.*, bipyridines, imidazolates, or carboxylates) can be viable due to the difference in their basicity. Such selective SALE, though not realized yet, can potentially open up new possibilities in preparing isoreticular MOFs with spatially controllable pore functionality.

Similarly, we speculate the future utility of BBR can conceptually encompass the following areas:

(i) BBR in MOF membranes: MOF membranes are regarded as interesting materials for gas separations.[14,122–128] However, the formation of MOF membranes is limited by synthetic obstacles (related to solvothermal MOF synthesis and preparation of a good quality membrane)[122,124,126,127,129] and the incorporation of desired functionality is also challenging. In this view, BBR in MOF membranes, especially ZIF-containing systems,[128–132] could offer new possibilities for enhancing the stability and versatility of separations.

(ii) BBR in Layer-by-Layer (LbL)-grown MOF films; the LbL technique has become a promising methodology for growing MOF films, with precise control over thickness, orientation, and porosity, on various substrates.[25,122] BBR in combination with LbL could significantly widen the scope of the LbL approach by application of post-LbL SALE or transmetalation, leading to multifunctional MOF films that are difficult to synthesize *de novo*.

(iii) Different attachment chemistry for non-bridging, charge compensating ligand exchange (SALI): exploration of different attachment chemistry for SALI is another way forward for the synthesis of highly robust functional MOFs (*vide supra*). This new concept could be further expanded in several directions by incorporation of various types of charged anchoring moieties (not limited to carboxylic acids) resulting in a broader scope of SALI. Utilizing this approach might lead to interesting directions such as incorporation of multiple light harvesters or redox active moieties for the construction of functional arrays or photoredox antenna systems.

While it is clear that SALE, transmetalation and non-bridging ligand exchange stand to become essential components in the MOF synthesis toolbox, it is also clear that much work is needed to fully understand many of the fundamental aspects governing these unique chemical transformations. Looking forward we anticipate that BBR will become a key player in the conversion of protoMOF structures that contain entirely new linkers and nodes and that those materials will exhibit unique properties that are rarely attainable utilizing traditional synthetic methods.

List of abbreviations

abp	4,4′-Azobis(pyridine)
AD	Alkanedioic acid
adn	Adeninate
bbta	Benzobistriazolate

bdc	Benzene dicarboxylate
bdcppi	*N,N′*-Bis(3,5-dicarboxylphenyl)pyromellitic diimide
bodipy	Boron dipyrromethene
brim	4-Bromoimidazolate
Br-tcpb	1,4-Dibromo-2,3,5,6-tetrakis(4-carboxyphenyl)benzene
btb	4,4′,4″-Benzene-1,3,5-triyl-tribenzoate
btc	Benzene-1,3,5-tricarboxylate
btdd	Bis(1,2,3-triazolate-[4,5-*b*],[4′,5′-*i*])dibenzo-[1,4]-dioxin
btin	Benzene-1,3,5-triyltriisonicotinate
btp	1,3,5-Benzenetriphosphonate
btt	1,3,5-Benzenetristetrazolate
bipy	4,4′-Bipyridine
bpdc	4,4′-Diphenyldicarboxylate
bpt	Biphenyl-3,4′,5-tricarboxylate
bpy	2,2′-Bipyridine
CdIF	Cadmium imidazolate framework
dabco	Triethylenediamine
dcbdt	1,4-Dicarboxylbenzene-2,3-dithiolate
dcim	4,5-Dichloroimidazolate
DEF	*N,N′*-Diethylformamide
DMF	*N,N′*-Dimethylformamide
dobdc	2,5-Dioxido-1,4-benzenedicarboxylate
dped	*meso*-1,2-Di(4-pyridyl)-1,2ethanediol
dpni	*N,N′*-Di-4-pyridylnaphthalene tetracarboxydiimide
eim	2-Ethylimidazolate
hbtc	Monoprotonated benzene-1,3,5-tricarboxylate
hett	5,5′,10,10′,15,15′-Hexaethayltruxene-2,7,12-tricarboxylate
H_4BDCPPI	*N,N′*-Bis(3,5-dicarboxyphenyl) pyromellitic diimide
H_2-hmcem	2-Hydroxymethyl-4,6-bi(2′-methoxyl-4′-(2″-1″-carboxyl)-ethylene)-1,3,5-mesitylene
HKUST	Hong Kong University of Science and Technology
ICP	Inductively coupled plasma
im	Imidazolate
LMCT	Ligand-to-metal charge transfer
MeOH	Methanol
MFU	Metal–organic framework Ulm University
MIL	Materials Institute Lavoisier
mim	2-Methylimidazolate
MOM	Metal–organic material
MSO	Metal salen octopus
ndc	2,6-Naphthalenedicarboxylate
NH_2-tpdc	2′-Amino-1,1′:4,1″-terphenyl-4,4″-dicarboxylate
nim	Nitroimidazole
NMR	Nuclear magnetic resonance
NU	Northwestern University
PAH	Polyaromatic hydrocarbon
PCMOF	Proton conducting metal–organic framework
PMOF	Polyhedron-based metal–organic framework
ppbotctc	*N*-Phenyl-*N′*-phenyl bicyclo[2,2,2]oct-7-ene-2,3,5,6-tetracarboxydiimide tetracarboxylic acid
PPF	Porphyrin paddlewheel framework
PXRD	Powder X-ray diffraction
RPM	Robust porphyrinic material
SALE	Solvent-assisted linker exchange
SALEM	Solvent-assisted linker exchanged material
salen	(*R*,*R*)-(−)-1,2-Cyclohexanediamino-*N*,*N′*-bis(3-*tert*-butyl-5-(4-pyridyl)salicylidene)$Mn^{III}Cl$
SALI	Solvent-assisted ligand insertion
SBU	Structural building unit
SNU	Seoul National University
SUMOF	Stockholm University metal–organic framework
TBAPy	1,3,6,8-Tetrakis(*p*-benzoate)pyrene
tcpb	2,3,5,6-Tetrakis(4-carboxyphenyl)benzene
tdpeb	1,3,5-Tris(3,5-dicarboxylphenylethynyl)benzene
thbts	2,4,6-Trihydroxy-1,3,5-benzenetrisulfonate
tmbbp	2,3,5,6-Tetramethyl-1,4-bis(4-pyridyl)benzene
tmbebp	2,3,5,6-Tetramethyl-1,4-bis-ethynyl-(4-pyridyl)-benzene
Zn-tcpp	Tetrakis(4-carboxyphenyl)porphyrinatozinc(II)
UiO	Universitetet i Oslo
ZIF	Zeolitic imidazolate framework

Acknowledgements

For support of our own work on building-block replacement chemistry we gratefully acknowledge U.S. Dept. of Energy, Office of Science, Basic Energy Sciences Program (chemical separations and synthesis methods development), the Stanford Global Climate and Energy Project (carbon capture), the Defense Threat Reduction Agency (degradation and capture of chemical threats), the U.S. Army Research Office (capture of toxic industrial chemicals), the U.S. Dept. of Energy, ARPA-E (methane storage and release); the Northwestern University Institute for Chemistry in Energy Processes (energy-related chemical catalysis), and the Institute for Sustainability and Energy at Northwestern (equipment acquisition). WB acknowledges support from the Foundation for Polish Science through the ''Kolumb'' Program.

Notes and references

1 G. Férey, Hybrid Porous Solids: Past, Present, Future, *Chem. Soc. Rev.*, 2008, **37**, 191–214.
2 O. M. Yaghi, M. O'Keefe, N. W. Ockwig, H. K. Chae, M. Eddaoudi and J. Kim, Reticular Synthesis and the Design of New Materials, *Nature*, 2003, **423**, 705–714.
3 S. Horike, S. Shimomura and S. Kitagawa, Soft Porous Crystals, *Nat. Chem.*, 2009, **1**, 695–704.
4 S. Kitagawa, R. Kitaura and S.-i. Noro, Functional Porous Coordination Polymers, *Angew. Chem., Int. Ed.*, 2004, **43**, 2334–2375.
5 H. Furukawa, K. E. Cordova, M. O'Keeffe and O. M. Yaghi, The Chemistry and Applications of Metal-Organic Frameworks, *Science*, 2013, **341**, 1230444.
6 O. K. Farha, A. Ö. Yazaydin, I. Eryazici, C. D. Malliakas, B. G. Hauser, M. G. Kanatzidis, S. T. Nguyen, R. Q. Snurr and J. T. Hupp, *De Novo* Synthesis of a Metal–Organic Framework Material Featuring Ultrahigh Surface Area and Gas Storage Capacities, *Nat. Chem.*, 2010, **2**, 944–948.

7 O. K. Farha, I. Eryazici, N. C. Jeong, B. G. Hauser, C. E. Wilmer, A. A. Sarjeant, R. Q. Snurr, S. T. Nguyen, A. Ö. Yazaydin and J. T. Hupp, Metal–Organic Framework Materials with Ultrahigh Surface Areas: Is the Sky the Limit?, *J. Am. Chem. Soc.*, 2012, **134**, 15016–15021.
8 D. Yuan, D. Zhao, D. Sun and H.-C. Zhou, An Isoreticular Series of Metal–Organic Frameworks with Dendritic Hexacarboxylate Ligands and Exceptionally High Gas-Uptake Capacity, *Angew. Chem., Int. Ed.*, 2010, **49**, 5357–5361.
9 H. Furukawa, N. Ko, Y. B. Go, N. Aratani, S. B. Choi, E. Choi, A. Ö. Yazaydin, R. Q. Snurr, M. O'Keeffe, J. Kim and O. M. Yaghi, Ultrahigh Porosity in Metal-Organic Frameworks, *Science*, 2010, **329**, 424–428.
10 C. E. Wilmer, O. K. Farha, T. Yildirim, I. Eryazici, V. Krungleviciute, A. A. Sarjeant, R. Q. Snurr and J. T. Hupp, Gram-Scale, High-Yield Synthesis of a Robust Metal–Organic Framework for Storing Methane and other Gases, *Energy Environ. Sci.*, 2013, **6**, 1158–1163.
11 C. E. Wilmer, O. K. Farha, Y.-S. Bae, J. T. Hupp and R. Q. Snurr, Structure–Property Relationships of Porous Materials for Carbon Dioxide Separation and Capture, *Energy Environ. Sci.*, 2012, **5**, 9849–9856.
12 L. J. Murray, M. Dincă and J. R. Long, Hydrogen Storage in Metal–Organic Frameworks, *Chem. Soc. Rev.*, 2009, **38**, 1294–1314.
13 J.-R. Li, R. J. Kuppler and H.-C. Zhou, Selective Gas Adsorption and Separation in Metal–Organic Frameworks, *Chem. Soc. Rev.*, 2009, **38**, 1477–1504.
14 K. Sumida, D. L. Rogow, J. A. Mason, T. M. McDonald, E. D. Bloch, Z. R. Herm, T.-H. Bae and J. R. Long, Carbon Dioxide Capture in Metal–Organic Frameworks, *Chem. Rev.*, 2012, **112**, 724–781.
15 M. P. Suh, H. J. Park, T. K. Prasad and D.-W. Lim, Hydrogen Storage in Metal–Organic Frameworks, *Chem. Rev.*, 2012, **112**, 782–835.
16 J.-R. Li, J. Sculley and H.-C. Zhou, Metal–Organic Frameworks for Separations, *Chem. Rev.*, 2012, **112**, 869–932.
17 Y. Peng, V. Krungleviciute, I. Eryazici, J. T. Hupp, O. K. Farha and T. Yildirim, Methane Storage in Metal–Organic Frameworks: Current Records, Surprise Findings, and Challenges, *J. Am. Chem. Soc.*, 2013, **135**, 11887–11894.
18 J. Lee, O. K. Farha, J. Roberts, K. A. Scheidt, S. T. Nguyen and J. T. Hupp, Metal-Organic Framework Materials as Catalysts, *Chem. Soc. Rev.*, 2009, **38**, 1450–1459.
19 L. Ma, C. Abney and W. Lin, Enantioselective Catalysis with Homochiral Metal–Organic Frameworks, *Chem. Soc. Rev.*, 2009, **38**, 1248–1256.
20 M. Yoon, R. Srirambalaji and K. Kim, Homochiral Metal–Organic Frameworks for Asymmetric Heterogeneous Catalysis, *Chem. Rev.*, 2012, **112**, 1196–1231.
21 C. A. Kent, D. Liu, L. Ma, J. M. Papanikolas, T. J. Meyer and W. Lin, Light Harvesting in Microscale Metal–Organic Frameworks by Energy Migration and Interfacial Electron Transfer Quenching, *J. Am. Chem. Soc.*, 2011, **133**, 12940–12943.
22 C. A. Kent, B. P. Mehl, L. Ma, J. M. Papanikolas, T. J. Meyer and W. Lin, Energy Transfer Dynamics in Metal-Organic Frameworks, *J. Am. Chem. Soc.*, 2010, **132**, 12767–12769.
23 S. Jin, H.-J. Son, O. K. Farha, G. P. Wiederrecht and J. T. Hupp, Energy Transfer from Quantum Dots to Metal–Organic Frameworks for Enhanced Light Harvesting, *J. Am. Chem. Soc.*, 2013, **135**, 955–958.
24 H.-J. Son, S. Jin, S. Patwardhan, S. J. Wezenberg, N. C. Jeong, M. So, C. E. Wilmer, A. A. Sarjeant, G. C. Schatz, R. Q. Snurr, O. K. Farha, G. P. Wiederrecht and J. T. Hupp, Light-Harvesting and Ultrafast Energy Migration in Porphyrin-Based Metal–Organic Frameworks, *J. Am. Chem. Soc.*, 2013, **135**, 862–869.
25 M. So, S. Jin, H.-J. Son, G. P. Wiederrecht, O. K. Farha and J. T. Hupp, Layer-by-Layer Fabrication of Oriented Porous Thin Films Based on Porphyrin-Containing Metal–Organic Frameworks, *J. Am. Chem. Soc.*, 2013, **135**, 15698–15701.
26 L. E. Kreno, K. Leong, O. K. Farha, M. Allendorf, R. P. Van Duyne and J. T. Hupp, Metal–Organic Framework Materials as Chemical Sensors, *Chem. Rev.*, 2012, **112**, 1105–1125.
27 Y. Cui, Y. Yue, G. Qian and B. Chen, Luminescent Functional Metal–Organic Frameworks, *Chem. Rev.*, 2012, **112**, 1126–1162.
28 C.-Y. Sun, X.-L. Wang, X. Zhang, C. Qin, P. Li, Z.-M. Su, D.-X. Zhu, G.-G. Shan, K.-Z. Shao, H. Wu and J. Li, Efficient and tunable white-light emission of metal–organic frameworks by iridium-complex encapsulation, *Nat. Commun.*, 2013, **4**, 2717.
29 S. Horike, D. Umeyama and S. Kitagawa, Ion Conductivity and Transport by Porous Coordination Polymers and Metal-Organic Frameworks, *Acc. Chem. Res.*, 2013, **46**, 2376–2384.
30 A. Shigematsu, T. Yamada and H. Kitagawa, Wide Control of Proton Conductivity in Porous Coordination Polymers, *J. Am. Chem. Soc.*, 2011, **133**, 2034–2036.
31 M. L. Aubrey, R. Ameloot, B. M. Wiers and J. R. Long, Metal–Organic Frameworks as Solid Magnesium Electrolytes, *Energy Environ. Sci.*, 2014, **7**, 667–671.
32 G. K. H. Shimizu, J. M. Taylor and S. Kim, Proton Conduction with Metal-Organic Frameworks, *Science*, 2013, **341**, 354–355.
33 C. Wang, T. Zhang and W. Lin, Rational Synthesis of Noncentrosymmetric Metal–Organic Frameworks for Second-Order Nonlinear Optics, *Chem. Rev.*, 2012, **112**, 1084–1104.
34 A. Hu, H. L. Ngo and W. Lin, Chiral Porous Hybrid Solids for Practical Heterogeneous Asymmetric Hydrogenation of Aromatic Ketones, *J. Am. Chem. Soc.*, 2003, **125**, 11490–11491.
35 D. W. Lewis, A. R. Ruiz-Salvador, A. Gomez, L. M. Rodriguez-Albelo, F.-X. Coudert, B. Slater, A. K. Cheetham and C. Mellot-Draznieks, Zeolitic Imidazole Frameworks: Structural and Energetics Trends Compared with their Zeolite Analogues, *CrystEngComm*, 2009, **11**, 2272–2276.

36 M. Eddaoudi, J. Kim, N. Rosi, D. Vodak, J. Wachter, M. O'Keefe and O. M. Yaghi, Systematic Design of Pore Size and Functionality in Isoreticular MOFs and Their Application in Methane Storage, *Science*, 2002, **295**, 469–472.

37 H. Deng, C. J. Doonan, H. Furukawa, R. B. Ferreira, J. Towne, C. B. Knobler, B. Wang and O. M. Yaghi, Multiple Functional Groups of Varying Ratios in Metal-Organic Frameworks, *Science*, 2010, **327**, 846–850.

38 S. M. Cohen, Postsynthetic Methods for the Functionalization of Metal–Organic Frameworks, *Chem. Rev.*, 2012, **112**, 970–1000.

39 K. K. Tanabe and S. M. Cohen, Postsynthetic Modification of Metal–Organic Frameworks—a Progress Report, *Chem. Soc. Rev.*, 2011, **40**, 498–519.

40 A. D. Burrows, in *Metal Organic Frameworks as Heterogeneous Catalysts*, ed. F. L. i. Xamena and J. Gascon, The Royal Society of Chemistry, 2013, pp. 31–75.

41 A. M. Shultz, A. A. Sarjeant, O. K. Farha, J. T. Hupp and S. T. Nguyen, Post-Synthesis Modification of a Metal–Organic Framework To Form Metallosalen-Containing MOF Materials, *J. Am. Chem. Soc.*, 2011, **133**, 13252–13255.

42 T. Gadzikwa, O. K. Farha, C. D. Malliakas, M. G. Kanatzidis, J. T. Hupp and S. T. Nguyen, Selective Bifunctional Modification of a Non-catenated Metal-Organic Framework Material *via* "Click" Chemistry, *J. Am. Chem. Soc.*, 2009, **131**, 13613–13615.

43 T. Gadzikwa, G. Lu, C. L. Stern, S. R. Wilson, J. T. Hupp and S. T. Nguyen, Covalent Surface Modification of a Metal–Organic Framework: Selective Surface Engineering *via* Cu^{I}-Catalyzed Huisgen Cycloaddition, *Chem. Commun.*, 2008, 5493–5495.

44 H. Sato, R. Matsuda, K. Sugimoto, M. Takata and S. Kitagawa, Photoactivation of a Nanoporous Crystal for On-Demand Guest Trapping and Conversion, *Nat. Mater.*, 2010, **9**, 661–666.

45 K. L. Mulfort and J. T. Hupp, Alkali Metal Cation Effects on Hydrogen Uptake and Binding in Metal-Organic Frameworks, *Inorg. Chem.*, 2008, **47**, 7936–7938.

46 O. K. Farha, K. L. Mulfort and J. T. Hupp, An Example of Node-Based Postassembly Elaboration of a Hydrogen-Sorbing, Metal–Organic Framework Material, *Inorg. Chem.*, 2008, **47**, 10223–10225.

47 Y. K. Hwang, D.-Y. Hong, J.-S. Chang, S. H. Jhung, Y.-K. Seo, J. Kim, A. Vimont, M. Daturi, C. Serre and G. Férey, Amine Grafting on Coordinatively Unsaturated Metal Centers of MOFs: Consequences for Catalysis and Metal Encapsulation, *Angew. Chem., Int. Ed.*, 2008, **47**, 4144–4148.

48 T. M. McDonald, D. M. D'Alessandro, R. Krishna and J. R. Long, Enhanced Carbon Dioxide Capture upon Incorporation of N,N′-Dimethylethylenediamine in the Metal–Organic Framework CuBTTri, *Chem. Sci.*, 2011, **2**, 2022–2028.

49 J. S. Seo, D. Whang, H. Lee, S. I. Jun, J. Oh, Y. J. Jeon and K. Kim, A Homochiral Metal-Organic Porous Material for Enantioselective Separation and Catalysis, *Nature*, 2000, **404**, 982–986.

50 S.-T. Zheng, X. Zhao, S. Lau, A. Fuhr, P. Feng and X. Bu, Entrapment of Metal Clusters in Metal–Organic Framework Channels by Extended Hooks Anchored at Open Metal Sites, *J. Am. Chem. Soc.*, 2013, **135**, 10270–10273.

51 R. Ameloot, M. Aubrey, B. M. Wiers, A. P. Gómora-Figueroa, S. N. Patel, N. P. Balsara and J. R. Long, Ionic Conductivity in the Metal–Organic Framework UiO-66 by Dehydration and Insertion of Lithium tert-Butoxide, *Chem. – Eur. J.*, 2013, **19**, 5533–5536.

52 M. Meilikhov, K. Yusenko and R. A. Fischer, Turning MIL-53(Al) Redox-Active by Functionalization of the Bridging OH-Group with 1,1′-Ferrocenediyl-Dimethylsilane, *J. Am. Chem. Soc.*, 2009, **131**, 9644–9645.

53 J. E. Mondloch, W. Bury, D. Fairen-Jimenez, S. Kwon, E. J. DeMarco, M. H. Weston, A. A. Sarjeant, S. T. Nguyen, P. C. Stair, R. Q. Snurr, O. K. Farha and J. T. Hupp, Vapor-Phase Metalation by Atomic Layer Deposition in a Metal–Organic Framework, *J. Am. Chem. Soc.*, 2013, **135**, 10294–10297.

54 C. Larabi and E. A. Quadrelli, Titration of $Zr_3(\mu\text{-OH})$ Hydroxy Groups at the Cornerstones of Bulk MOF UiO-67, $[Zr_6O_4(OH)_4(\text{biphenyldicarboxylate})_6]$, and Their Reaction with $[AuMe(PMe_3)]$, *Eur. J. Inorg. Chem.*, 2012, 3014–3022.

55 O. Karagiaridi, W. Bury, A. A. Sarjeant, C. L. Stern, O. K. Farha and J. T. Hupp, Synthesis and Characterization of Isostructural Cadmium Zeolitic Imidazolate Frameworks *via* Solvent-Assisted Linker Exchange, *Chem. Sci.*, 2012, **3**, 3256–3260.

56 O. Karagiaridi, W. Bury, E. Tylianakis, A. A. Sarjeant, J. T. Hupp and O. K. Farha, Opening Metal–Organic Frameworks Vol. 2: Inserting Longer Pillars into Pillared-Paddlewheel Structures through Solvent-Assisted Linker Exchange, *Chem. Mater.*, 2013, **25**, 3499–3503.

57 O. Karagiaridi, M. B. Lalonde, W. Bury, A. A. Sarjeant, O. K. Farha and J. T. Hupp, Opening ZIF-8: A Catalytically Active Zeolitic Imidazolate Framework of Sodalite Topology with Unsubstituted Linkers, *J. Am. Chem. Soc.*, 2012, **134**, 18790–18796.

58 M. Lalonde, W. Bury, O. Karagiaridi, Z. Brown, J. T. Hupp and O. K. Farha, Transmetalation: Routes to Metal Exchange within Metal–Organic Frameworks, *J. Mater. Chem. A*, 2013, **1**, 5453–5468.

59 M. Kim, J. F. Cahill, Y. Su, K. A. Prather and S. M. Cohen, Postsynthetic Ligand Exchange as a Route to Functionalization of 'Inert' Metal–Organic Frameworks, *Chem. Sci.*, 2012, **3**, 126–130.

60 M. Kondo, S. Furukawa, K. Hirai and S. Kitagawa, Coordinatively Immobilized Monolayers on Porous Coordination Polymer Crystals, *Angew. Chem., Int. Ed.*, 2010, **49**, 5327–5330.

61 N. Yanai and S. Granick, Directional Self-Assembly of a Colloidal Metal–Organic Framework, *Angew. Chem., Int. Ed.*, 2012, **51**, 5638–5641.

62 X. Song, S. Jeong, D. Kim and M. S. Lah, Transmetalations in Two Metal–Organic Frameworks with Different Framework Flexibilities: Kinetics and Core–Shell Heterostructure, *CrystEngComm*, 2012, **14**, 5753–5756.

63 X. Song, T. K. Kim, H. Kim, D. Kim, S. Jeong, H. R. Moon and M. S. Lah, Post-Synthetic Modifications of Framework Metal Ions in Isostructural Metal–Organic Frameworks: Core–Shell Heterostructures *via* Selective Transmetalations, *Chem. Mater.*, 2012, **24**, 3065–3073.

64 B. J. Burnett, P. M. Barron, C. Hu and W. Choe, Stepwise Synthesis of Metal–Organic Frameworks: Replacement of Structural Organic Linkers, *J. Am. Chem. Soc.*, 2011, **133**, 9984–9987.

65 S. Kim, K. W. Dawson, B. S. Gelfand, J. M. Taylor and G. K. H. Shimizu, Enhancing Proton Conduction in a Metal–Organic Framework by Isomorphous Ligand Replacement, *J. Am. Chem. Soc.*, 2013, **135**, 963–966.

66 M. Kim, J. F. Cahill, H. Fei, K. A. Prather and S. M. Cohen, Postsynthetic Ligand and Cation Exchange in Robust Metal–Organic Frameworks, *J. Am. Chem. Soc.*, 2012, **134**, 18082–18088.

67 W. Bury, D. Fairen-Jimenez, M. B. Lalonde, R. Q. Snurr, O. K. Farha and J. T. Hupp, Control over Catenation in Pillared Paddlewheel Metal–Organic Framework Materials *via* Solvent-Assisted Linker Exchange, *Chem. Mater.*, 2013, **25**, 739–744.

68 H. Fei, J. F. Cahill, K. A. Prather and S. M. Cohen, Tandem Postsynthetic Metal Ion and Ligand Exchange in Zeolitic Imidazolate Frameworks, *Inorg. Chem.*, 2013, **52**, 4011–4016.

69 A. F. Gross, E. Sherman, S. L. Mahoney and J. J. Vajo, Reversible Ligand Exchange in a Metal–Organic Framework (MOF): Toward MOF-Based Dynamic Combinatorial Chemical Systems, *J. Phys. Chem. A*, 2013, **117**, 3771–3776.

70 S. Takaishi, E. J. DeMarco, M. J. Pellin, O. K. Farha and J. T. Hupp, Solvent-Assisted Linker Exchange (SALE) and Post-Assembly Metallation in Porphyrinic Metal–Organic Framework Materials, *Chem. Sci.*, 2013, **4**, 1509–1513.

71 L.-H. Wang, R. Shang, Z. Zheng, C.-L. Liu and Z.-M. Wang, Two Systems of $[DabcoH_2]^{2+}$/$[PipH_2]^{2+}$–Uranyl–Oxalate Showing Reversible Crystal-to-Crystal Transformations Controlled by the Diammonium/Uranyl/Oxalate Ratios in Aqueous Solutions ($[DabcoH_2]^{2+}$ = 1,4-Diazabicyclo-[2.2.2]-octaneH_2 and $[PipH_2]^{2+}$ = PiperazineH_2), *Cryst. Growth Des.*, 2013, **13**, 2597–2606.

72 N. A. Vermeulen, O. Karagiaridi, A. A. Sarjeant, C. L. Stern, J. T. Hupp, O. K. Farha and J. F. Stoddart, Aromatizing Olefin Metathesis by Ligand Isolation inside a Metal–Organic Framework, *J. Am. Chem. Soc.*, 2013, **135**, 14916–14919.

73 S. Pullen, H. Fei, A. Orthaber, S. M. Cohen and S. Ott, Enhanced Photochemical Hydrogen Production by a Molecular Diiron Catalyst Incorporated into a Metal–Organic Framework, *J. Am. Chem. Soc.*, 2013, **135**, 16997–17003.

74 S. Jeong, D. Kim, X. Song, M. Choi, N. Park and M. S. Lah, Postsynthetic Exchanges of the Pillaring Ligand in Three-Dimensional Metal–Organic Frameworks, *Chem. Mater.*, 2013, **25**, 1047–1054.

75 G. Alberti, E. Giontella and S. Murcia-Mascarós, Mechanism of the Formation of Organic Derivatives of γ-Zirconium Phosphate by Topotactic Reactions with Phosphonic Acids in Water and Water–Acetone Media, *Inorg. Chem.*, 1997, **36**, 2844–2849.

76 H. R. Allcock and G. Y. Moore, Synthesis of Poly(organophosphazene) Copolymers and Cross-Linked Polymers by Ligand Exchange, *Macromolecules*, 1972, **5**, 231–232.

77 J.-R. Li and H.-C. Zhou, Bridging-Ligand-Substitution Strategy for the Preparation of Metal–Organic Polyhedra, *Nat. Chem.*, 2010, **2**, 893–898.

78 M. Ziegler, A. V. Davis, D. W. Johnson and K. N. Raymond, Supramolecular Chirality: A Reporter of Structural Memory, *Angew. Chem., Int. Ed.*, 2003, **42**, 665–668.

79 T. Li, M. T. Kozlowski, E. A. Doud, M. N. Blakely and N. L. Rosi, Stepwise Ligand Exchange for the Preparation of a Family of Mesoporous MOFs, *J. Am. Chem. Soc.*, 2013, **135**, 11688–11691.

80 D. Peralta, G. Chaplais, A. Simon-Masseron, K. Barthelet, C. Chizallet, A.-A. Quoineaud and G. D. Pirngruber, Comparison of the Behavior of Metal–Organic Frameworks and Zeolites for Hydrocarbon Separations, *J. Am. Chem. Soc.*, 2012, **134**, 8115–8126.

81 G. A. N. Felton, A. K. Vannucci, J. Chen, L. T. Lockett, N. Okumura, B. J. Petro, U. I. Zakai, D. H. Evans, R. S. Glass and D. L. Lichtenberger, Hydrogen Generation from Weak Acids: Electrochemical and Computational Studies of a Diiron Hydrogenase Mimic, *J. Am. Chem. Soc.*, 2007, **129**, 12521–12530.

82 D. Streich, Y. Astuti, M. Orlandi, L. Schwartz, R. Lomoth, L. Hammarström and S. Ott, High-Turnover Photochemical Hydrogen Production Catalyzed by a Model Complex of the [FeFe]-Hydrogenase Active Site, *Chem. – Eur. J.*, 2010, **16**, 60–63.

83 Y. Inokuma, M. Kawano and M. Fujita, Crystalline Molecular Flasks, *Nat. Chem.*, 2011, **3**, 349–358.

84 P. Deria, J. E. Mondloch, E. Tylianakis, P. Ghosh, W. Bury, R. Q. Snurr, J. T. Hupp and O. K. Farha, Perfluoroalkane Functionalization of NU-1000 *via* Solvent-Assisted Ligand Incorporation: Synthesis and CO_2 Adsorption Studies, *J. Am. Chem. Soc.*, 2013, **135**, 16801–16804.

85 P. Deria, W. Bury, J. T. Hupp and O. K. Farha, Versatile Functionalization of the NU-1000 Platform by Solvent-Assisted Ligand Incorporation, *Chem. Commun.*, 2014, **50**, 1965–1968.

86 H. Wu, T. Yildirim and W. Zhou, Exceptional Mechanical Stability of Highly Porous Zirconium Metal–Organic Framework UiO-66 and Its Important Implications, *J. Phys. Chem. Lett.*, 2013, **4**, 925–930.

87 H. Wu, Y. S. Chua, V. Krungleviciute, M. Tyagi, P. Chen, T. Yildirim and W. Zhou, Unusual and Highly Tunable Missing-Linker Defects in Zirconium Metal-Organic Framework UiO-66 and Their Important Effects on Gas Adsorption, *J. Am. Chem. Soc.*, 2013, **135**, 10525–10532.

88 M. J. Katz, Z. J. Brown, Y. J. Colón, P. W. Siu, K. A. Scheidt, R. Q. Snurr, J. T. Hupp and O. K. Farha, A Facile Synthesis of UiO-66, UiO-67 and their Derivatives, *Chem. Commun.*, 2013, **49**, 9449–9451.

89 D. H. Hong and M. P. Suh, Enhancing CO_2 Separation Ability of a Metal-Organic Framework by Post-Synthetic Ligand Exchange with Flexible Aliphatic Carboxylates, *Chem. – Eur. J.*, 2014, **20**, 426–434.

90 S. Das, H. Kim and K. Kim, Metathesis in Single Crystal: Complete and Reversible Exchange of Metal Ions Constituting the Frameworks of Metal–Organic Frameworks, *J. Am. Chem. Soc.*, 2009, **131**, 3814–3815.

91 T. K. Prasad, D. H. Hong and M. P. Suh, High Gas Sorption and Metal-Ion Exchange of Microporous Metal–Organic Frameworks with Incorporated Imide Groups, *Chem. – Eur. J.*, 2010, **16**, 14043–14050.

92 C. K. Brozek and M. Dincă, Lattice-Imposed Geometry in Metal-Organic Frameworks: Lacunary Zn_4O Clusters in **MOF-5** Serve as Tripodal Chelating Ligands for Ni^{2+}, *Chem. Sci.*, 2012, **3**, 2110–2113.

93 C. K. Brozek and M. Dincă, Ti^{3+}-, $V^{2+/3+}$-, $Cr^{2+/3+}$-, Mn^{2+}-, and Fe^{2+}-Substituted MOF-5 and Redox Reactivity in Cr- and Fe-MOF-5, *J. Am. Chem. Soc.*, 2013, **135**, 12886–12891.

94 D. Denysenko, T. Werner, M. Grzywa, A. Puls, V. Hagen, G. Eickerling, J. Jelic, K. Reuter and D. Volkmer, Reversible Gas-Phase Redox Processes Catalyzed by Co-Exchanged MFU-4*l*(arge), *Chem. Commun.*, 2012, **48**, 1236–1238.

95 M. Dincă and J. R. Long, High-Enthalpy Hydrogen Adsorption in Cation-Exchanged Variants of the Microporous Metal–Organic Framework $Mn_3[(Mn_4Cl)_3(BTT)_8(CH_3OH)_{10}]_2$, *J. Am. Chem. Soc.*, 2007, **129**, 11172–11176.

96 C. H. Lau, R. Babarao and M. R. Hill, A Route to Drastic Increase of CO_2 Uptake in Zr Metal Organic Framework UiO-66, *Chem. Commun.*, 2013, **49**, 3634–3636.

97 J. Kahr, R. E. Morris and P. A. Wright, Post-synthetic incorporation of nickel into CPO-27(Mg) to give materials with enhanced permanent porosity, *CrystEngComm*, 2013, **15**, 9779–9786.

98 J.-H. Liao, W.-T. Chen, C.-S. Tsai and C.-C. Wang, Characterization, Adsorption Properties, Metal Ion-Exchange and Crystal-to-Crystal Transformation of $Cd_3[(Cd_4Cl)_3(BTT)_8(H_2O)_{12}]_2$ Framework, where BTT^{3-} = 1,3,5-Benzenetristetrazolate, *CrystEngComm*, 2013, **15**, 3377–3384.

99 G. Mukherjee and K. Biradha, Post-Synthetic Modification of Isomorphic Coordination Layers: Exchange Dynamics of Metal Ions in a Single Crystal to Single Crystal Fashion, *Chem. Commun.*, 2012, **48**, 4293–4295.

100 H.-M. Zhang, J. Yang, Y.-C. He and J.-F. Ma, An Unusual Porous Metal–Organic Framework that Demonstrates the Highly Efficient Exchange of Metal Ions and the Reversible Adsorption of Iodine, *Chem. – Asian J.*, 2013, **8**, 2787–2791.

101 Q. Yao, J. Sun, K. Li, J. Su, M. V. Peskov and X. Zou, A Series of Isostructural Mesoporous Metal–Organic Frameworks Obtained by Ion-Exchange Induced Single-Crystal to Single-Crystal Transformation, *Dalton Trans.*, 2012, **41**, 3953–3955.

102 T.-T. Lian, S.-M. Chen, F. Wangb and J. Zhang, Metal–Organic Framework Architecture with Polyhedron-in-Polyhedron and Further Polyhedral Assembly, *CrystEngComm*, 2013, **15**, 1036–1038.

103 Z. Zhang, W.-Y. Gao, L. Wojtas, S. Ma, M. Eddaoudi and M. J. Zaworotko, Post-Synthetic Modification of Porphyrin-Encapsulating Metal–Organic Materials by Cooperative Addition of Inorganic Salts to Enhance CO_2/CH_4 Selectivity, *Angew. Chem., Int. Ed.*, 2012, **51**, 9330–9334.

104 Z. Zhang, L. Zhang, L. Wojtas, P. Nugent, M. Eddaoudi and M. J. Zaworotko, Templated Synthesis, Postsynthetic Metal Exchange, and Properties of a Porphyrin-Encapsulating Metal–Organic Material, *J. Am. Chem. Soc.*, 2011, **134**, 924–927.

105 Z.-J. Zhang, W. Shi, Z. Niu, H.-H. Li, B. Zhao, P. Cheng, D.-Z. Liao and S.-P. Yan, A New Type of Polyhedron-Based Metal–Organic Frameworks with Interpenetrating Cationic and Anionic Nets Demonstrating Ion Exchange, Adsorption and Luminescent Properties, *Chem. Commun.*, 2011, **47**, 6425–6427.

106 J. Li, L. Li, H. Hou and Y. Fan, Study on the Reaction of Polymeric Zinc Ferrocenyl Carboxylate with Pb(II) or Cd(II), *Cryst. Growth Des.*, 2009, **9**, 4504–4513.

107 L. Mi, H. Hou, Z. Song, H. Han and Y. Fan, Polymeric Zinc Ferrocenyl Sulfonate as a Molecular Aspirator for the Removal of Toxic Metal Ions, *Chem. – Eur. J.*, 2008, **14**, 1814–1821.

108 L. Mi, H. Hou, Z. Song, H. Han, H. Xu, Y. Fan and S.-W. Ng, Rational Construction of Porous Polymeric Cadmium Ferrocene-1,1′-disulfonates for Transition Metal Ion Exchange and Sorption, *Cryst. Growth Des.*, 2007, **7**, 2553–2561.

109 S. Huang, X. Li, X. Shi, H. Hou and Y. Fan, Structure Extending and Cation Exchange of Cd(II) and Co(II) Materials Compounds Inducing Fluorescence Signal Mutation, *J. Mater. Chem.*, 2010, **20**, 5695–5699.

110 Z. Wei, W. Lu, H.-L. Jiang and H.-C. Zhou, A Route to Metal–Organic Frameworks through Framework Templating, *Inorg. Chem.*, 2013, **52**, 1164–1166.

111 D. Feng, Z.-Y. Gu, J.-R. Li, H.-L. Jiang, Z. Wei and H.-C. Zhou, Zirconium-Metalloporphyrin PCN-222: Mesoporous Metal–Organic Frameworks with Ultrahigh Stability as Biomimetic Catalysts, *Angew. Chem., Int. Ed.*, 2012, **51**, 10307–10310.

112 J. A. Botas, G. Calleja, M. Sánchez-Sánchez and M. G. Orcajo, Cobalt Doping of the MOF-5 Framework and Its Effect on Gas-Adsorption Properties, *Langmuir*, 2010, **26**, 5300–5303.

113 C. J. Kepert and M. J. Rosseinsky, Zeolite-Like Crystal Structure of an Empty Microporous Molecular Framework, *Chem. Commun.*, 1999, 375–376.

114 O. M. Yaghi, H. Li, C. Davis, D. Richardson and T. L. Groy, Synthetic Strategies, Structure Patterns, and Emerging Properties in the Chemistry of Modular Porous Solids, *Acc. Chem. Res.*, 1998, **31**, 474–484.

115 A. P. Nelson, O. K. Farha, K. L. Mulfort and J. T. Hupp, Supercritical Processing as a Route to High Internal Surface Areas and Permanent Microporosity in Metal-Organic

Framework Materials, *J. Am. Chem. Soc.*, 2009, **131**, 458–460.

116 J. A. Mason, M. Veenstra and J. R. Long, Evaluating Metal–Organic Frameworks for Natural Gas Storage, *Chem. Sci.*, 2014, **5**, 32–51.

117 C.-X. Yang, H.-B. Ren and X.-P. Yan, Fluorescent Metal–Organic Framework MIL-53(Al) for Highly Selective and Sensitive Detection of Fe^{3+} in Aqueous Solution, *Anal. Chem.*, 2013, **85**, 7441–7446.

118 In a MIL-53 coordination environment, Fe(III) should be relatively easy to reduce. If so, then rapid luminescence quenching by electron transfer from photo-excited BDC to Fe(III) would account qualitatively for the observations. If the photo-prepared molecular exciton can migrate from linker to linker (for example, *via* Förster energy transfer) only a comparatively small fraction of the Al(III) ions would need to be displaced by Fe(III) in order to engender fluorescence quenching. Although no evidence for or against such amplified quenching is presented in the original report, it's occurrence might account for the observed low Fe(III) detection threshold.

119 R. D. Shannon, Revised Effective Ionic Radii and Systematic Studies of Interatomic Distances in Halides and Chalcogenides, *Acta Crystallogr., Sect. A*, 1976, **32**, 751–767.

120 K. Tan, N. Nijem, P. Canepa, Q. Gong, J. Li, T. Thonhauser and Y. J. Chabal, Stability and Hydrolyzation of Metal Organic Frameworks with Paddle-Wheel SBUs upon Hydration, *Chem. Mater.*, 2012, **24**, 3153–3167.

121 X. Kong, H. Deng, F. Yan, J. Kim, J. A. Swisher, B. Smit, O. M. Yaghi and J. A. Reimer, Mapping of Functional Groups in Metal-Organic Frameworks, *Science*, 2013, **341**, 882–885.

122 A. Bétard and R. A. Fischer, Metal–Organic Framework Thin Films: From Fundamentals to Applications., *Chem. Rev.*, 2012, **112**, 1055–1083.

123 J. Gascon and F. Kapteijn, Metal-Organic Framework Membranes—High Potential, Bright Future?, *Angew. Chem., Int. Ed.*, 2010, **49**, 1530–1532.

124 H. Guo, G. Zhu, I. J. Hewitt and S. Qiu, "Twin Copper Source" Growth of Metal–Organic Framework Membrane: $Cu_3(BTC)_2$ with High Permeability and Selectivity for Recycling H_2, *J. Am. Chem. Soc.*, 2009, **131**, 1646–1647.

125 M. Arnold, P. Kortunov, D. J. Jones, Y. Nedellec, J. Kärger and J. Caro, Oriented Crystallisation on Supports and Anisotropic Mass Transport of the Metal-Organic Framework Manganese Formate, *Eur. J. Inorg. Chem.*, 2007, 60–64.

126 D. Zacher, O. Shekhah, C. Wöll and R. A. Fischer, Thin Films of Metal–Organic Frameworks, *Chem. Soc. Rev.*, 2009, **38**, 1418–1429.

127 O. Shekhah, J. Liu, R. A. Fischer and C. Wöll, MOF Thin Films: Existing and Future Applications, *Chem. Soc. Rev.*, 2011, **40**, 1081–1106.

128 S. Aguado, C.-H. Nicolas, V. Moizan-Baslé, C. Nieto, H. Amrouche, N. Bats, N. Audebrand and D. Farrusseng, Facile Synthesis of an Ultramicroporous MOF Tubular Membrane With Selectivity Towards CO_2, *New J. Chem.*, 2011, **35**, 41–44.

129 O. Shekhah, R. Swaidan, Y. Belmabkhout, M. d. Plessis, T. Jacobs, L. J. Barbour, I. Pinnau and M. Eddaoudi, The Liquid Phase Epitaxy Approach for the Successful Construction of Ultra-Thin and Defect-Free ZIF-8 Membranes: Pure and Mixed Gas Transport Study, *Chem. Commun.*, 2014, **50**, 2089–2092.

130 H. Bux, F. Liang, Y. Li, J. Cravillon, M. Wiebcke and J. Caro, Zeolitic Imidazolate Framework Membrane with Molecular Sieving Properties by Microwave-Assisted Solvothermal Synthesis, *J. Am. Chem. Soc.*, 2009, **131**, 16000–16001.

131 Y.-S. Li, H. Bux, A. Feldhoff, G.-L. Li, W.-S. Yang and J. Caro, Controllable Synthesis of Metal–Organic Frameworks: From MOF Nanorods to Oriented MOF Membranes, *Adv. Mater.*, 2010, **22**, 3322–3326.

132 A. Huang, H. Bux, F. Steinbach and J. Caro, Molecular-Sieve Membrane with Hydrogen Permselectivity: ZIF-22 in LTA Topology Prepared with 3-Aminopropyltriethoxysilane as Covalent Linker, *Angew. Chem., Int. Ed.*, 2010, **49**, 4958–4961.

